Thermodynamic characterization of the (CO_2 + O_2) binary system for the development of models for CCS processes: Accurate experimental (p, ρ, T) data and virial coefficients

Daniel Lozano-Martín[1], David Vega-Maza[1], M. Carmen Martín[1], Dirk Tuma[2], and César R. Chamorro[1].

[1] Grupo de Termodinámica y Calibración (TERMOCAL), Research Institute on Bioeconomy, Escuela de Ingenierías Industriales, Universidad de Valladolid, Paseo del Cauce, 59, E-47011 Valladolid, Spain.

[2] BAM Bundesanstalt für Materialforschung und -prüfung, D-12200 Berlin, Germany.

https://doi.org/10.1016/j.supflu.2020.105074

Abstract

Continuing our study on (CO_2 + O_2) mixtures, this work reports new experimental (p, ρ, T) data for two oxygen-rich mixtures with mole fractions $x(O_2)$ = (0.50 and 0.75) mol·mol^{-1}, in the temperature range T = (250 to 375) K and pressure range p = (0.5 to 20) MPa, using a single-sinker densimeter. Experimental density data were compared to two well established equation-of-state models: EOS-CG and GERG-2008. In the p, T-range investigated, the EOS-CG gave a better reproduction for the equimolar mixture ($x(O_2)$ = 0.5), whereas the GERG-2008 performed significantly better for the oxygen-rich mixture ($x(O_2)$ = 0.75). The EOS-CG generally overestimates the density, while the GERG-2008 underestimates it. This complete set of new experimental data, together with previous measurements, is used to calculate the virial coefficients $B(T, x)$ and $C(T, x)$, as well as the second interaction virial coefficient $B_{12}(T)$ for the (CO_2 + O_2) system.

Keywords: carbon capture and storage (CCS); density of binary mixtures (CO_2 + O_2); gravimetric preparation; single-sinker densimeter; virial coefficients.

* Corresponding author e-mail: cescha@eii.uva.es. Tel.: +34 983423756. Fax: +34 983423363

1. Introduction

High-accuracy density data are of great relevance for the development of reliable equations of state. In part one of this study [1], we reported accurate density measurements for three binary mixtures of carbon dioxide with oxygen (amount-of-substance fraction $x(O_2)$ = 0.05, 0.10, 0.20) in the temperature range T = (250 to 375) K and maximum pressures up to p = 13 MPa, together with the corresponding calculations using the two equation-of-state models GERG-2008 [2] and EOS-CG [3]. It could be observed that the GERG-2008 EoS fitted the experimental data within its claimed uncertainty in density (1 %) only for the mixture with the lowest oxygen content (amount-of-substance fraction $x(O_2)$ = 0.05). When the oxygen content increased ($x(O_2)$ = 0.10, 0.20), the deviations increased above the claimed uncertainty of the EoS and became more visible at lower temperatures and higher pressures. These deviations could be as high as 4.4 % for the mixture with $x(O_2)$ = 0.10, and 6.6 % for the mixture with $x(O_2)$ = 0.20. The deviations always had a positive value, i.e., the GERG-2008 underestimates the density of (CO_2 + O_2) mixtures, particularly for mixtures with a high oxygen content at high pressures and low temperatures. Another result of that study was that the EOS-CG performed much better in processing these density data. The relative deviations of the experimental density data from the EOS-CG remained within the claimed uncertainty of the equation of state (1 %) for all the 162 experimental points, with three exceptions only, namely at ($x(O_2)$ = 0.10, T = 293.15 K, p = 6.0 MPa), ($x(O_2)$ = 0.20, T = 300 K, p = 11.0 MPa), and ($x(O_2)$ = 0.20, T = 300 K, p = 12.2 MPa), where the relative deviation increased up to 1.2 %, −2.0 %, and −3.2 %, respectively.

In order to complete the characterization of the (CO_2 + O_2) binary mixture over the entire composition range, accurate density measurements for two new binary mixtures with higher oxygen content ($x(O_2)$ = 0.50, 0.75) are presented in this work. Measurements were performed at temperatures between (250 and 375) K and pressures up to 20 MPa using a single-sinker densimeter with magnetic suspension coupling, which is the same experimental technique used in the previous work. In order to achieve the highest accuracy in composition, the binary mixtures for this investigation were also prepared gravimetrically according to the ISO 6142-1 [4], a method that qualifies for the production of reference materials. The

experimental results were compared with the GERG-2008 equation of state as well as with the more specific EOS-CG.

The complete set of density data for the binary system (CO_2 + O_2) presented in this work, and in the previous work [1], covers a wide range of temperature (from T = 250 K to T = 375 K), pressure (up to p = 20 MPa), and composition (from $x(O_2)$ = 0.05 to $x(O_2)$ = 0.75). This complete set of new experimental data from both studies is used in this work to calculate the virial coefficients $B(T, x)$ and $C(T, x)$, as well as the second interaction virial coefficient $B_{12}(T)$ for the (CO_2 + O_2) binary mixture.

The characterization of the binary system (CO_2 + O_2) is relevant not only for the development of accurate models for Carbon Capture and Storage (CCS) processes and for the modeling of combustion processes, but also for the improvement of the models used when dealing with natural gas and natural-gas-related mixtures. The deviations of the theoretical models from the actual values of the thermodynamic properties of the mixtures have relevant implications in the design and operation of processes and in the commercial transfer and pricing of products.

2. Experimental

2.1. Mixture preparation

Two (CO_2 + O_2) binary mixtures were prepared at the Federal Institute for Materials Research and Testing (Bundesanstalt für Materialforschung und -prüfung, BAM) in Berlin, Germany, according to the ISO 6142-1 [4].

Purity, supplier, molar mass, and critical parameters of the pure compounds (obtained from the reference equations of state for carbon dioxide [5] and oxygen [6]) are given in Table 1. The cylinder identifiers (BAM reference gas mixture G 033), the gravimetric composition, and the corresponding expanded uncertainty (k = 2) of the mixtures are set out in Table 2. The prepared mixtures were supplied in aluminum cylinders with a volume of 10 dm^3. The entire mixture preparation procedure was executed in the same way as described in part one of this study [1]. Carbon dioxide and oxygen were used without further purification, but information on impurities from the specification by the supplier was considered in the mixture preparation.

Here, the following gas portions were determined that resulted in the final pressures:

Cylinder 1009-180717 ($x(O_2) = 0.50$): 1331.724 g CO_2 968.171 g O_2 $p = 13.5$ MPa

Cylinder 1099-180717 ($x(O_2) = 0.75$): 667.386 g CO_2 1455.068 g O_2 $p = 13.6$ MPa

The cylinders were also validated at BAM by gas chromatography using the same procedures as before [1]. Due to the composition of the mixtures, unlike part one, the analyzed compound was CO_2 in both cases. The results of the GC analysis and the composition of the mixtures used for validation are given in Table 3.

2.2. Equipment description

As in the previous work [1], the (p, ρ, T) data were measured using a single-sinker magnetic suspension densimeter (SSMSD) especially designed for density measurements of pure gases and gaseous mixtures. Details of the equipment and measurement procedure have previously been described by Chamorro et al. [7], Mondéjar et al. [8], and Lozano-Martín et al. [9]. This method, originally developed by Brachthäuser et al. [10] and improved by Klimeck et al. [11], operates on the Archimedes principle. A magnetic suspension coupling system allows the buoyancy force on a sinker immersed in the gas to be determined, so accurate density measurements of fluids over wide temperature and pressure ranges can be obtained. The setting of the equipment and the installed devices can be found in [12].

2.3. Density measurement procedure

The procedures for measuring densities are the same as in part one of this study [1], where the corresponding details can be found. Additional details of the measurement procedure in SSMSD are presented by Mondéjar et al. [8] and Lozano-Martín et al. [9] for our equipment and by McLinden [13] and Richter and Kleinrahm [14] on general aspects. In a simplified way, the density of the fluid can be calculated from Eq. (1):

$$\rho_{\text{fluid}} = \frac{m_{s0} - m_{sf}}{V_s(T,p)} \quad (1)$$

where the difference between the result of weighing the sinker in a vacuum m_{s0} and in the pressurized fluid m_{sf} is related to the buoyancy force exerted on the sinker. It is determined using a high-precision microbalance. V_s (T, p) is the volume of the sinker immersed in the fluid, whose dependence on temperature and pressure is accurately known [8].

As explained in the previous work [1], the calibration of the balance and the correction due to the force transmission error (FTE) were considered [9][15], while the mass-based magnetic susceptibilities χ_s for the two (CO_2 + O_2) binary mixtures studied in this work were estimated using the additive law proposed by Bitter [16].

2.4. Experimental procedure

Experimental density data for the two (CO_2 + O_2) binary mixtures (x(O_2) = 0.50 and 0.75) were obtained at temperatures of (250, 260, 275, 293.15, 300, 325, 350, and 375) K and pressures up to 20 MPa, always in the gas phase, whose limits are previously calculated with the EOS-CG [3] in order to always remain at pressures well below the saturation curve for each temperature. In the same way as applied in part one, the pressure was reduced in 1 MPa steps from the highest measured pressure to 1 MPa for each isotherm during a measurement campaign. The coordinates in Figure 1 show the recorded data in a p, T-diagram together with the saturation curve for the mixture calculated with the EOS-CG [3]. Additionally, the p, T-range of applicability of the EOS-CG and the relevant area of interest for CCS applications are also indicated in the two plots of Figure 1.

Each individual coordinate was evaluated from thirty repeated measurements of each single (p, ρ, T) point and the last ten values are used to obtain the mean value. The balance calibration factor α is obtained right before and after every single point, and the apparatus-specific effect Φ_0 is determined at the end of every single isotherm.

To minimize sorption effects inside the measuring cell, which may cause errors up to 0.1 % in density, the measuring cell was evacuated and flushed several times with fresh mixture before the isotherm is started,

as recommended by Richter and Kleinrahm [14]. The residence time of the mixture in the cell never exceeded 40 hours. In this study, specific sorption tests for this particular mixture were performed in the same way as in previous works [12], [17]–[27]. Continuous density measurements on the same state point were recorded over 48 hours to detect any drifting. The results showed that the difference observed in the trend of the relative deviation in density between the measured and the calculated densities, using GERG-2008 EoS for these calculations, between the first and last measurements of one campaign are one order of magnitude lower than the density uncertainty achievable with the equipment. A measurement with fresh mixture executed immediately afterwards, for the same temperature and pressure, reproduced the density value with a deviation of one order of magnitude lower than the density uncertainty of the equipment. Consequently, residual errors due to sorption effects are not discernible with the experimental technique, and it should be considered that they are already included in the measurement uncertainty of the density and in the uncertainty in composition.

2.5. Uncertainty of the measurements

A detailed analysis of the uncertainties of the measurements involved in this experimental procedure was reported in previous works [8][9]. The quantities which contribute to the uncertainty of the measurements in this study are as follows:

The expanded uncertainty in temperature ($k = 2$) is less than 4 mK. The pressure uncertainty depends on the range and is given by Eq. (2) and Eq. (3) for the (3 to 20) MPa and (0 to 3) MPa transducers, respectively. The expanded uncertainty ($k = 2$) in pressure is in both cases less than 0.005 MPa.

$$U(p)/\mathrm{MPa} = 75\cdot10^{-6}\cdot p/\mathrm{MPa} + 3.5\cdot10^{-3} \quad (2)$$

$$U(p)/\mathrm{MPa} = 60\cdot10^{-6}\cdot p/\mathrm{MPa} + 1.7\cdot10^{-3} \quad (3)$$

The uncertainty of density data for the two (CO_2 + O_2) binary mixtures investigated, corrected by both the apparatus-specific and the fluid-specific FTE effects, $U(\rho_{\mathrm{fluid}})$, is evaluated according to the methods

proposed in the Guide to the Expression of Uncertainty in Measurement (GUM) [28]. Eq. (4) is the working equation used in this study, where χ_s stands for the mass-based magnetic susceptibility.

$$U(\rho)/\mathrm{kg\cdot m^{-3}} = 2.5\cdot 10^{4}\cdot \chi_s/\mathrm{m^3\cdot kg^{-1}} + 1.1\cdot 10^{-4}\cdot \rho/\mathrm{kg\cdot m^{-3}} + 2.3\cdot 10^{-2} \quad (4)$$

The resulting working equation (Eq. (5)) to calculate the overall expanded uncertainty in density $U_T(\rho)$ (k = 2) includes uncertainties of density, temperature, pressure, and composition of the mixture.

$$U_T(\rho) = 2\cdot\left[u(\rho)^2 + \left(\left(\frac{\partial\rho}{\partial p}\right)_{T,x}\cdot u(p)\right)^2 + \left(\left(\frac{\partial\rho}{\partial T}\right)_{p,x}\cdot u(T)\right)^2 + \sum_i \left(\left(\frac{\partial\rho}{\partial x_i}\right)_{T,p,x_j\neq x_i}\cdot u(x_i)\right)^2\right]^{0.5} \quad (5)$$

In Eq. (5), p is the pressure, T is the temperature, and x_i is the amount-of-substance (mole) fraction of each mixture component. Partial derivatives were calculated from the GERG-2008 EoS using the REFPROP software [29].

The individual contributions of density, temperature, pressure, and composition to the overall uncertainty in density for the three studied (CO_2 + O_2) binary mixtures are given in Table 4.

3. Experimental results

Tables 5 and 6 show the 274 experimental (p, ρ, T) data measured for the two (CO_2 + O_2) binary mixtures. The temperature, pressure, and density of each measured point were calculated as the arithmetic mean of the last ten consecutive measurements of a series of thirty. Tables 5 and 6 also show the expanded uncertainty in density $U(\rho_{exp})$ (k = 2), calculated by Eq. (4) and expressed in absolute density units and as a percentage of the measured density.

The experimental data were compared to the corresponding densities calculated from the two equations of state GERG-2008 and EOS-CG using the REFPROP [29] and TREND 4.0 [30] software. Relative deviations of the experimental densities from the corresponding EoS-values are included in Tables 5 and 6 and are shown in Figures 2 and 3.

The densities of the experimental points recorded in this work range from ρ = 9.294 kg·m^{-3} (T = 250 K, p = 0.5 MPa, $x(O_2)$ = 0.50) to ρ = 536.87 kg·m^{-3} (T = 275 K, p = 18.8 MPa, $x(O_2)$ = 0.50).

Note that analogously to part one of this study, there is a correction applied due to the fluid-specific effect originating from the content of a paramagnetic fluid, namely oxygen. This correction can be applied thanks to the estimation of the apparatus-specific constant ε_ρ of the fluid-specific effect in a previous work [9]. The contribution of this correction is much higher for the mixtures measured in this work, as the oxygen content is much higher. In fact, the correction due to the fluid-specific effect can be as high as 6.701 kg·m^{-3} in absolute value (1.49 % relative value), at the highest density of ρ = 448.577 kg·m^{-3}; or as high as 2.13 % in relative value (0.368 kg·m^{-3} absolute value), at the lowest density of ρ = 17.245 kg·m^{-3}, for the mixture with the higher oxygen content (0.25 CO_2 + 0.75 O_2) at T = 250 K.

4. Discussion of the results

4.1. Relative deviation of the experimental data from the reference equations of state

The plot in Figure 2 shows the relative deviations of the experimentally determined density data of the (0.50 CO_2 + 0.50 O_2) mixture from the corresponding density data calculated by the GERG-2008 (a) and the EOS-CG (b) models, respectively. In the same way, Figure 3 shows the deviations for the (0.25 CO_2 + 0.75 O_2) mixture.

Both equations of state claim an uncertainty in density of 1.0 % for mixtures of CO_2 and O_2 over the temperature range from (250 to 450) K and at pressures up to 35 MPa. The estimated uncertainty of experimental density data ranges from 0.019 % for T = 275 K, p = 18.8 MPa (ρ = 536.87 kg·m^{-3}) for the (0.50 CO_2 + 0.50 O_2) mixture to 0.377 % for T = 375 K, p = 1.0 MPa (ρ = 11.262 kg·m^{-3}) for the (0.25 CO_2 + 0.75 O_2) mixture. A slightly bigger relative uncertainty of 0.438 % can be found in a single point for the (0.50 CO_2 + 0.50 O_2) mixture at T = 250 K, but this value is due to the fact that this point is the only one that has been measured at the pressure of p = 0.5 MPa, with a density as low as 9.294 kg·m^{-3}.

The relative deviations of the experimental density data from the corresponding data of GERG-2008 (Figures 2 (a) and 3 (a)) are larger for the mixture with lower oxygen content, i.e., the (0.50 CO_2 + 0.50 O_2) mixture. Here, 55 of the 123 experimental points deviate more than the claimed uncertainty of the

equation of state. This behavior emerges for all the measured temperatures except the two highest at T = 350 K and T = 375 K, respectively. The relative deviations can be as large as 3.90 %. For the mixture with the higher oxygen content, i.e., the (0.25 CO_2 + 0.75 O_2) mixture, only 2 of the 151 measured points (at T = 250 K, and p = 10.0 MPa and p = 11.0 MPa) deviate slightly more (1.05 %) than the claimed uncertainty of the EoS. These two points are close to the saturation curve, as can be seen in Figure 1(b). Almost all the deviations have a positive value which means that the GERG-2008 EoS underestimates the density of (CO_2 + O_2) mixtures. Further, the course of the deviation is not monotonous. With increasing pressures, the curves pass a maximum and the deviation diminishes towards the maximum pressure of 20 MPa. This maximum is located at approximately 10 MPa for the (0.25 CO_2 + 0.75 O_2) mixture, whereas, for the (0.50 CO_2 + 0.50 O_2) mixture, higher temperatures shift this maximum deviation towards higher pressures.

In contrast to the GERG-2008, the relative deviations of the experimental density data from the corresponding data of the EOS-CG increase as the oxygen content in the mixture increases. For the (0.50 CO_2 + 0.50 O_2) mixture, 23 of the 123 experimental points deviate more than the claimed uncertainty of the EOS-CG (Figure 3 (b)). This occurs for temperatures of 275 K, 293.15 K, and 300 K and pressures higher than 10 MPa. The relative deviations reach a maximum of –2.95 %. For the mixture with the higher oxygen content, i.e., the (0.25 CO_2 + 0.75 O_2) mixture, 33 of the 151 measured points deviate more than the claimed uncertainty of the EOS-CG (Figure 4 (b)). This region is entered for pressures over 9 MPa at T = 250 K, over 10 MPa at T = 260 K, over 12 MPa at T = 275 K, over 15 MPa at T = 293.15 K, and only over 18 MPa at T = 300 K. Here, the relative deviations can be as large as –2.64 %. The larger deviations always have a negative value, i.e., the EOS-CG overestimates the density of (CO_2 + O_2), being more pronounced for mixtures with high oxygen content, at high pressures and low temperatures, and the slope of the curve displays a minimum. In reverse analogy to the GERG-2008, higher temperatures move this minimum towards higher pressures.

4.2 Virial coefficients

The virial coefficients for the five (CO_2 + O_2) mixtures, the three measured in the previous work ($x(O_2)$ = 0.05, 0.10, and 0.20) [1] and the two measured in this work ($x(O_2)$ = 0.50 and 0.75), were calculated by fitting the experimental density data to the virial EoS:

$$\frac{p}{RT} = \sum_{k=1}^{N} \frac{B_k}{M^k} \rho_{\text{exp}}^k \quad (6)$$

where p is the pressure, T is the temperature, R is the molar gas constant, ρ_{exp} is the experimental density, M is the molar mass, and B_k with k = 1, 2, … (B_1 = 1) are the second, third,… virial coefficients, respectively.

The method proposed by Cristancho *et al*. [31] was used to determine the number of terms at which the virial EoS must be truncated and the maximum density ρ_{max} of the experimental points used to fit this equation. The procedure, described in detail in a previous work [23], consists of two consecutive fits. Both fits were executed using a least-squares fitting method implemented in MATLAB software [32].

The first fit determines the number of virial coefficients N needed for the best representation of the experimental data and the maximum density ρ_{max} for which the fit gives a satisfying result. This is done through the determination of the apparent molar mass M of the mixture as a parameter of the virial EoS, while varying the number of coefficients of the virial EoS N and the range of the experimental data sets until the obtained value of M is as close as possible to the accepted reference value of M for each mixture. The first fit is performed under the following conditions: that the number of experimental points to be fitted is higher than $2 \cdot N$, the standard uncertainty of all the virial coefficients is lower than their own value (then, the parameters are significant), and the root mean square of the residuals is within the expanded (k = 2) experimental uncertainty in density.

The first fit yielded that the closest values of M are obtained with a third order (N = 3) of the virial EoS for all the compositions and temperatures. The value of ρ_{max} is between (117.407 and 153.813) kg·m^{-3} ($p \approx$ 7 to 8 MPa) for the (0.95 CO_2 + 0.05 O_2) mixture, between (123.409 and 231.402) kg·m^{-3} ($p \approx$ 5 to 7 MPa) for the (0.90 CO_2 + 0.10 O_2) mixture, between (118.408 and 264.364) kg·m^{-3} ($p \approx$ 7 to 9 MPa) for the (0.80 CO_2 + 0.20 O_2) mixture, between (146.474 and 426.654) kg·m^{-3} ($p \approx$ 11 to 19 MPa) for the (0.50

CO_2 + 0.50 O_2) mixture, and lastly between (127.886 and 332.575) kg·m^{-3} ($p \approx 11$ to 15 MPa) for the (0.25 CO_2 + 0.75 O_2) mixture. For some isotherms, it was not possible to obtain a regression complying with the three conditions indicated above for all studied compositions. The virial coefficients at the lowest temperatures, T = (250 and 260) K, were only obtained for the mixture with the higher oxygen content (0.25 CO_2 + 0.75 O_2), and the virial coefficients at T = 275 K were only obtained for the two mixtures with higher oxygen content, (0.50 CO_2 + 0.50 O_2) and (0.25 CO_2 + 0.75 O_2). This is because these relatively low-temperature isotherms fall just below the phase envelopes for the mixtures with lower oxygen content (and thus, high carbon dioxide content) and the explored experimental range includes no more than 5 points to a rather low ρ_{max} of 109.732 kg·m^{-3} (at T = 275 K, p = 3.94 MPa for the (0.95 CO_2 + 0.05 O_2) mixture)

The second fit calculates the values of the corresponding virial coefficients, using the values of N and ρ_{max} obtained in the first fit. The final calculus is performed with the value of M fixed to the accepted reference value for each mixture. The results for the second $B(T, x)$ and third $C(T, x)$ virial coefficients are reported in Table 7 for all the five binary (CO_2 + O_2) mixtures of this work, together with their uncertainty determined by the Monte Carlo method [33]. Three points were treated as outliers and they are reported neither in Table 7 nor in Figure 4, namely those at T = 375 K for the (0.95 CO_2 + 0.05 O_2) mixture and at T = 350 K for the (0.95 CO_2 + 0.05 O_2) and (0.90 CO_2 + 0.10 O_2) mixtures.

Table 7 and Figures 4 and 5 also report the second interaction virial coefficients B_{12} obtained from the second virial coefficients using the reference EoS of pure carbon dioxide B_{11} [5], pure oxygen B_{22} [6], and the expression:

$$B(T,x) = x_1^2 B_{11}(T) + 2x_1 x_2 B_{12}(T) + x_2^2 B_{22}(T) \quad (7)$$

where x_1 and x_2 are the mole fraction of carbon dioxide and oxygen, respectively. The expanded (k = 2) uncertainty of B_{12} has been determined applying the law of uncertainty propagation [28] to the uncertainties of the mixture's second virial coefficient B from the Monte Carlo method, as described above, and the uncertainties of B_{11} (0.5 cm^3·mol^{-1}) and B_{22} (0.3 cm^3·mol^{-1}) from [34].

The second interaction virial coefficients B_{12} for the binary (CO_2 + O_2) system investigated in our studies were fitted to:

$$B_{12} = N_0 + \frac{N_1}{T} \quad (8)$$

with the corresponding parameters reported in Table 8. The residuals of the fit to Eq. (8) are plotted in Figure 5b, with a root mean square of 2.3 %, a value which remains within the 4.3 % average expanded (k = 2) uncertainty of B_{12}.

Figure 4 and Table 7 depict B_{12} as a function of the mole fraction of oxygen for each isotherm. As can be seen, the values computed from the EOS-CG show a dependence with the mixture composition, especially for the isotherms at the lowest temperatures, while the experimentally estimated values of B_{12} have a flatter trend with the composition, as stated by the theory. Thus, at a higher content of oxygen, the experimental results of B_{12} are less negative than the corresponding results evaluated from the EOS-CG. However, at the lowest mole fraction of oxygen, the behaviour is the opposite.

Figure 5a and Table 7 display the average value of B_{12} from all the compositions as a function of the temperature and a comparison with the values given by the GERG-2008 model, the EOS-CG model, and available data in the literature. There is good agreement between the EOS-CG and the experimental B_{12}, with deviations within the $U(B_{12,\,exp})$ = 4.3 %. Moreover, the experimental values of B_{12} are consistent, considering their respective uncertainties, with the literature data of Martin et al. [35] ($U(B_{12,\text{Martin et al.}})$ = 3.3 %) and Gorski and Miller [36] ($U(B_{12,\text{Gorski and Miller}})$ = 0.7 %). Nevertheless, there are larger discrepancies with the data of Edwards and Roseveare [37] ($U(B_{12,\text{Edwards and Roseveare}})$ = 5.3 %) and a different trend with temperature is found concerning the data of Cottrell et al. [38] ($U(B_{12,\text{Cottrell et al.}})$ = 17.0 %). Notably, the deviations from applying the GERG-2008 EoS are significant. The values of B_{12} obtained from the GERG-2008 EoS are significantly higher than those from the experiment. The deviations are one order of magnitude higher compared to those originating from the EOS-CG, ranging from 9 % up to 68 %, being far beyond the $U(B_{12,\,exp})$. This may be due to the fact that the binary system (CO_2 + O_2) in the GERG-2008 EoS is correlated only to binary vapor-liquid equilibrium data [39], while the EOS-CG also

considers density [36][40][41], speed of sound [42], and second interaction virial coefficient data sets [35, 38] to regress the model. Moreover, the EOS-CG uses more accurate EoS for pure carbon dioxide [5] and oxygen [6], instead of the expressions used in the GERG-2008 EoS for the same substances [43][44].

4.3. General analysis of the joint data for the five different compositions

Considering the results presented in this work together with the results presented in the previous work [1] as a whole, we can say that, in general, the EOS-CG can reproduce the experimental density data better than the GERG-2008 EoS. This can be seen clearly in Figure 6 (a) and (b). This is not surprising, as the EOS-CG is specifically designed for this kind of mixtures, whereas the GERG-2008 is a more general approach. However, strictly speaking, the EOS-CG fits the experimental data within its claimed uncertainty only for the mixtures with the lower oxygen content ($x(O_2)$ = 0.05, 0.10 and 0.20). For the mixtures with higher oxygen content ($x(O_2)$ = 0.50 and 0.75), mainly at high pressures (p > 10 MPa) and low temperatures (T < 300 K), the EOS-CG cannot reliably reproduce the experimental data within its claimed uncertainty. Unexpectedly, the GERG-2008 can fit the experimental data within the uncertainty borders for the mixture with the highest oxygen content ($x(O_2)$ = 0.75) better than the EOS-CG, which presents deviations as high as –2.64 %. The virial equation of state, with the coefficients obtained in this work, can reproduce the experimental data with greater precision, as can be seen in Figure 6 (c), where the relative deviations of the experimental pressure from the pressure given by the virial equation of state are plotted as a function of density. The deviations are very small and only for the higher values of density, i.e., above 400 $kg \cdot m^{-3}$, are the deviations bigger than 0.4 %, with a maximum deviation of 1.3 % for the (0.50 CO_2 + 0.50 O_2) mixture and 3.4 % for the (0.80 CO_2 + 0.20 O_2) mixture.

Table 9 presents the statistical parameters of the relative deviation of the experimental data from the densities given by the EOS-CG and the GERG-2008 and from pressures given by the virial equation of state. The AAD of experimental data from the densities calculated by the EOS-CG amounts to 0.077 % for the (0.95 CO_2 + 0.05 O_2) mixture, 0.15 % for the (0.90 CO_2 + 0.10 O_2) mixture, 0.22 % for the (0.80 CO_2 + 0.20 O_2) mixture, 0.59 % for the (0.50 CO_2 + 0.50 O_2) mixture, and 0.66 % for the (0.25 CO_2 + 0.75 O_2) mixture. The corresponding AAD of experimental data from the densities calculated by the GERG-2008 are 0.29 %, 0.69 %, 1.3 %, 1.2 %, and 0.32 %. Only for the most oxygen-rich (0.25 CO_2 + 0.75 O_2)

mixture is the AAD of the GERG-2008 smaller than that of the EOS-CG. The RMS of experimental data from the pressures given by the virial equation of state ranges between 0.035 % for the (0.95 CO_2 + 0.05 O_2) mixture and 0.47 % for the (0.80 CO_2 + 0.20 O_2) mixture.

The availability of data for (CO_2 + O_2) mixtures in the literature is limited to oxygen contents below $x(O_2)$ = 0.10 [40], [45][46][42][53][54]. For this reason, a direct comparison with these experimental data is difficult and will remain rather speculative. The data from these references were also processed to obtain the statistical parameters of the relative deviation of these experimental data from the densities calculated by the EOS-CG and the GERG-2008 and are given in Table 9.

Regarding the vapor-liquid equilibrium of the mixture, apart from being object of this work, it can be said, based on the analysis of available experimental data [39], [41], [47-50], that the (CO_2 + O_2) mixture is a Type I binary system according to the van Konynenburg and Scott classification [51]. This behavior is to be expected from a binary system of molecules of similar size, the absence of a dipole moment, and an average energy of the CO_2–O_2 interaction of the same order of magnitude to the average energy of CO_2–CO_2 and O_2–O_2 interactions in the mixture [52].

5. Conclusions

New (p, ρ, T) high-precision experimental data for two binary mixtures of carbon dioxide and oxygen, with nominal compositions of (0.50 CO_2 + 0.50 O_2) and (0.25 CO_2 + 0.75 O_2), at temperatures between (250 and 375) K and pressures up to 20 MPa, are reported. The gravimetrically prepared mixtures were of reference quality and the experimental device used was a single-sinker densimeter with magnetic suspension coupling.

The new experimental data were compared to the corresponding densities calculated from the EOS-CG and the GERG-2008 equation-of-state models and rated by the uncertainty threshold of 1 %, which is applicable for both models. The results of all five mixtures ($x(O_2)$ = 0.05, 0.10, 0.20, 0.50, and 0.75) investigated were employed to determine virial coefficients.

For the two mixtures under study here, in the p, T-range investigated, the equimolar mixture ($x(O_2)$ = 0.5) was better reproduced by the EOS-CG but the GERG-2008 performed better on the mixture with the

highest oxygen content ($x(O_2) = 0.75$). The EOS-CG also gave better results for the three carbon dioxide-rich mixtures investigated in part one of this study ($x(O_2) = 0.05$, 0.10, and 0.20) [1]. Generally, the GERG-2008 underestimated the density of all mixture compositions, while the deviations became larger towards lower temperatures and frequently surpassed the uncertainty threshold. In contrast to the GERG-2008, the relative deviations in density calculated by the EOS-CG did not show a distinct trend. There was no clear temperature dependence observed for the three carbon dioxide-rich mixtures and the values remained mostly within the uncertainty threshold over the entire p, T- range. For the other two mixtures, however, a tendency to underestimate the density was found, which became larger at lower temperatures and pressures > 10 MPa. Notably, the plot deviation versus pressure of both the GERG-2008 and the EOS-CG passed an extremum for several mixtures, namely the GERG-2008 on $x(O_2) = 0.20$ and both models on $x(O_2) = 0.50$ and 0.75.

The complete set of experimental data, which covers the entire composition range of the binary (CO_2 + O_2) mixture for the first time, together with the obtained virial coefficients, is an important tool to develop and improve the models and equations of state needed to design and operate processes with carbon dioxide and oxygen, such as CCS.

Acknowledgments

The authors wish to thank for their support the Ministerio de Economía, Industria y Competitividad project ENE2017-88474-R and the Junta de Castilla y León project VA280P18.

References

[1] D. Lozano-Martín, G. U. Akubue, A. Moreau, D. Tuma, and C. R. Chamorro, "Accurate experimental (p, ρ, T) data of the (CO_2 + O_2) binary system for the development of models for CCS processes," *J. Chem. Thermodyn.*, vol. 150, 106210, Nov. 2020, doi: 10.1016/j.jct.2020.106210.

[2] O. Kunz and W. Wagner, "The GERG-2008 Wide-Range Equation of State for Natural Gases and Other Mixtures: An Expansion of GERG-2004," *J. Chem. Eng. Data*, vol. 57, no. 11, pp. 3032–

3091, Nov. 2012, doi: 10.1021/je300655b.

[3] J. Gernert and R. Span, “EOS-CG: A Helmholtz energy mixture model for humid gases and CCS mixtures,” *J. Chem. Thermodyn.*, vol. 93, pp. 274–293, Feb. 2016, doi: 10.1016/j.jct.2015.05.015.

[4] International Organisation for Standardization, “ISO 6142-1:2015. Gas analysis - Preparation of calibration gas mixtures - Part 1: Gravimetric method for Class I mixtures,” Geneva, 2015.

[5] R. Span and W. Wagner, “A new equation of state for carbon dioxide covering the fluid region from the triple-point temperature to 1100 K at pressures up to 800 MPa,” *J. Phys. Chem. Ref. Data*, vol. 25, no. 6, pp. 1509-1596, 1996, doi: 10.1063/1.555991.

[6] R. Schmidt and W. Wagner, “A new form of the equation of state for pure substances and its application to oxygen,” *Fluid Phase Equilib.*, vol. 19, no. 3, 1985, doi: 10.1016/0378-3812(85)87016-3.

[7] C. R. Chamorro, J. J. Segovia, M. C. Martín, M. A. Villamañán, J. F. Estela-Uribe, and J. P. M. Trusler, “Measurement of the (pressure, density, temperature) relation of two (methane+nitrogen) gas mixtures at temperatures between 240 and 400 K and pressures up to 20 MPa using an accurate single-sinker densimeter,” *J. Chem. Thermodyn.*, vol. 38, no. 7, pp. 916–922, Jul. 2006, doi: 10.1016/j.jct.2005.10.004.

[8] M. E. Mondéjar, J. J. Segovia, and C. R. Chamorro, “Improvement of the measurement uncertainty of a high accuracy single sinker densimeter via setup modifications based on a state point uncertainty analysis,” *Measurement*, vol. 44, no. 9, pp. 1768–1780, Nov. 2011, doi: 10.1016/j.measurement.2011.07.012.

[9] D. Lozano-Martín, M. E. Mondéjar, J. J. Segovia, and C. R. Chamorro, “Determination of the force transmission error in a single-sinker magnetic suspension densimeter due to the fluid-specific effect and its correction for use with gas mixtures containing oxygen,” *Measurement*, vol. 151, art. no. 107176, Oct. 2019, doi: 10.1016/j.measurement.2019.107176.

[10] K. Brachthäuser, R. Kleinrahm, H. W. Lösch, and W. Wagner, “Entwicklung eines neuen Dichtemeßverfahrens und Aufbau einer Hochtemperatur-Hochdruck-Dichtemeßanlage,” *Entwicklung eines neuen Dichtemeßverfahrens und Aufbau einer Hochtemperatur-Hochdruck-Dichtemeßanlage*, no. 371, 1993.

[11] J. Klimeck, R. Kleinrahm, and W. Wagner, “An accurate single-sinker densimeter and measurements of the (*p*, *ρ*, *T*) relation of argon and nitrogen in the temperature range from (235 to 520) K at pressures up to 30 MPa,” *J. Chem. Thermodyn.*, vol. 30, no. 12, pp. 1571–1588, 1998, doi: 10.1006/jcht.1998.0421.

[12] R. Hernández-Gómez, D. Tuma, A. Gómez-Hernández, and C. R. Chamorro, “Accurate Experimental (p , ρ, T) Data for the Introduction of Hydrogen into the Natural Gas Grid: Thermodynamic Characterization of the Nitrogen–Hydrogen Binary System from 240 to 350 K and Pressures up to 20 MPa,” *J. Chem. Eng. Data*, vol. 62, no. 12, pp. 4310–4326, Dec. 2017, doi: 10.1021/acs.jced.7b00694.

[13] M. O. McLinden, “Experimental techniques 1: direct methods.,” in *Volume Properties – Liquids, Solutions and Vapours*, T. Wilhelm, E.; Letcher, Ed. Cambridge: Royal Society of Chemistry, 2015, pp. 73–79, doi: 10.1039/9781782627043-00073.

[14] M. Richter and R. Kleinrahm, “Influence of adsorption and desorption on accurate density measurements of gas mixtures,” *J. Chem. Thermodyn.*, vol. 74, pp. 58–66, Jul. 2014, doi: 10.1016/j.jct.2014.03.020.

[15] M. O. McLinden, R. Kleinrahm, and W. Wagner, “Force transmission errors in magnetic suspension densimeters,” *Int. J. Thermophys.*, vol. 28, no. 2, pp. 429–448, Apr. 2007, doi: 10.1007/s10765-007-0176-0.

[16] F. Bitter, “The Magnetic Susceptibilities of Several Organic Gases,” *Phys. Rev.*, vol. 33, no. 3, pp. 389–397, Mar. 1929, doi: 10.1103/PhysRev.33.389.

[17] R. Hernández-Gómez, T. Fernández-Vicente, D. del Campo, M. Vaľková, M. Chytil, and C. R. Chamorro, “Characterization of a biomethane-like synthetic gas mixture through accurate density measurements from (240 to 350) K and pressures up to 14 MPa,” *Fuel*, vol. 206, pp. 420-428, 2017, doi: 10.1016/j.fuel.2017.06.040.

[18] M. E. Mondéjar, M. C. Martín, R. Span, and C. R. Chamorro, “New (*p*, *ρ*, *T*) data for carbon dioxide – nitrogen mixtures from (250 to 400) K at pressures up to 20 MPa,” *J. Chem. Thermodyn.*, vol. 43, no. 12, pp. 1950–1953, Dec. 2011, doi: 10.1016/j.jct.2011.07.006.

[19] M. E. Mondéjar, R. M. Villamañán, R. Span, and C. R. Chamorro, “Accurate (*p*, *ρ*, *T*) data for two

new (carbon dioxide + nitrogen) mixtures from (250 to 400) K at pressures up to 20 MPa," *J. Chem. Thermodyn.*, vol. 48, pp. 254–259, May 2012, doi: 10.1016/j.jct.2011.12.035.

[20] R. Hernández-Gómez, T. E. Fernández-Vicente, M. C. Martín González, M. E. Mondéjar, and C. R. Chamorro, "Integration of biogas in the natural gas grid: Thermodynamic characterization of a biogas-like mixture," *J. Chem. Thermodyn.*, vol. 84, pp. 60–66, May 2015, doi: 10.1016/j.jct.2014.12.028.

[21] R. Hernández-Gómez, D. Tuma, J. J. Segovia, and C. R. Chamorro, "Experimental determination of (p, ρ, T) data for binary mixtures of methane and helium," *J. Chem. Thermodyn.*, vol. 96, pp. 1–11, Dec. 2015, doi: 10.1016/j.jct.2015.12.006.

[22] R. Hernandez-Gomez, D. Tuma, M.A. Villamañán, M.E. Mondéjar, and C.R. Chamorro, "Accurate thermodynamic characterization of a synthetic coal mine methane mixture," *J. Chem. Thermodyn.*, vol. 68, pp. 253–259, Jan. 2014, doi: 10.1016/j.jct.2013.09.023.

[23] R. Hernández-Gómez, D. Tuma, R. Villamañán, and C. R. Chamorro, "Accurate experimental (p, ρ, T) data and virial coefficients for the (methane and helium) binary system," *J. Chem. Thermodyn.*, vol. 101, pp. 168–179, May 2016, doi: 10.1016/j.jct.2016.05.024.

[24] R. Hernández-Gómez, D. Tuma, D. Lozano-Martín, and C. R. Chamorro, "Accurate experimental (p, ρ, T) data of natural gas mixtures for the assessment of reference equations of state when dealing with hydrogen-enriched natural gas," *Int. J. Hydrogen Energy*, vol. 43, no. 49, pp. 21983–21998, Dec. 2018, doi: 10.1016/j.ijhydene.2018.10.027.

[25] R. Hernández-Gómez, D. Tuma, E. Pérez, and C. R. Chamorro, "Accurate Experimental (p, ρ, and T) Data for the Introduction of Hydrogen into the Natural Gas Grid (II): Thermodynamic Characterization of the Methane–Hydrogen Binary System from 240 to 350 K and Pressures up to 20 MPa," *J. Chem. Eng. Data*, vol. 63, no. 5, pp. 1613–1630, May 2018, doi: 10.1021/acs.jced.7b01125.

[26] M. E. Mondéjar, T. E. Fernández-Vicente, F. Haloua, and C. R. Chamorro, "Experimental Determination of (p, ρ, T) Data for Three Mixtures of Carbon Dioxide with Methane for the Thermodynamic Characterization of Nonconventional Energy Gases," *J. Chem. Eng. Data*, vol. 57, no. 9, pp. 2581–2588, Sep. 2012, doi: 10.1021/je300665n.

[27] M. E. Mondéjar, M. A. Villamañán, R. Span, and C. R. Chamorro, "(p, ρ, T) Behavior of Two Mixtures of Carbon Monoxide with Nitrogen in the Temperature Range from (250 to 400) K and Pressures up to 20 MPa," *J. Chem. Eng. Data*, vol. 56, no. 10, pp. 3933–3939, Oct. 2011, doi: 10.1021/je2007764.

[28] Joint Comitee for Guides in Metrology, JCGM100:2008, and GUM1995, "Evaluation of measurement data — Guide to the expression of uncertainty in measurement," *JCGM 100:2008 GUM 1995 with Minor Correct.*, 2008.

[29] E. W. Lemmon, I. H. Bell, M. L. Huber, M. O. McLinden, "NIST Standard Reference Database 23: Reference Fluid Thermodynamic and Transport Properties-REFPROP, Version 10.0," Natl. Inst. Stand. Technol. Stand. Ref. Data Progr., 2018.

[30] R. Span, R. Beckmüller, T. Eckermann, S. Herrig, S. Hielscher, A. Jäger, E. Mickoleit, T. Neumann,S.M. Pohl, B. Semrau, M. Thol, "TREND. Thermodynamic Reference and Engineering Data 4.0. Lehrstuhl für Thermodynamik, Ruhr-Universität Bochum." 2019.

[31] D. E. Cristancho, P. L. Acosta-Perez, I. D. Mantilla, J. C. Holste, K. R. Hall, and G. A. Iglesias-Silva, "A Method To Determine Virial Coefficients from Experimental (p, ρ, T) Measurements," *J. Chem. Eng. Data*, vol. 60, no. 12, pp. 3682–3687, Dec. 2015, doi: 10.1021/acs.jced.5b00629.

[32] The MathWorks Inc., "MATLAB and Statistics Toolbox R2011a." Natick, Massachusetts, United States, 2011.

[33] BIPM, "Evaluation of measurement data — Supplement 1 to the 'Guide to the expression of uncertainty in measurement' — Propagation of distributions using a Monte Carlo method," *JCGM 101:2008*. 2008.

[34] M. Frenkel and K. N. Marsh, Eds., *Virial Coefficients of Pure Gases*, vol. 21A. Berlin/Heidelberg: Springer-Verlag, 2002.

[35] M.L. Martin, R.D. Trengove, K.R. Harris, and P.J. Dunlop, "Excess second virial coefficients for some dilute binary gas mixtures," *Aust. J. Chem.*, vol. 35, no. 8, p. 1525, 1982, doi: 10.1071/CH9821525.

[36] R. A. Gorski and J. G. Miller, "The Interaction Coefficients of Gas Mixtures" *J. Am. Chem. Soc.*, vol. 75, no. 3, pp. 550–552, Feb. 1953, doi: 10.1021/ja01099a011.

[37] A. E. Edwards and W. E. Roseveare, "The Second Virial Coefficients of Gaseous Mixtures" *J. Am. Chem. Soc.*, vol. 64, no. 12, pp. 2816–2819, Dec. 1942, doi: 10.1021/ja01264a028.

[38] T. L. Cottrell, R. A. Hamilton, and R. P. Taubinger, "The second virial coefficients of gases and mixtures. Part 2.—Mixtures of carbon dioxide with nitrogen, oxygen, carbon monoxide, argon and hydrogen," *Trans. Faraday Soc.*, vol. 52, pp. 1310–1312, 1956, doi: 10.1039/TF9565201310.

[39] A. Fredenslund and G. A. Sather, "Gas-Liquid Equilibrium of the Oxygen–Carbon Dioxide System," *J. Chem. Eng. Data*, vol. 15 (1), pp. 17–22, 1970, doi: 10.1021/je60044a024.

[40] M. Mantovani, P. Chiesa, G. Valenti, M. Gatti, and S. Consonni, "Supercritical pressure–density–temperature measurements on CO_2–N_2, CO_2–O_2 and CO_2–Ar binary mixtures," *J. Supercrit. Fluids*, vol.61, pp.34–43, 2011, doi: 10.1016/j.supflu.2011.09.001.

[41] N. K. Muirbrook and J. M. Prausnitz, "Multicomponent vapor–liquid equilibria at high pressures: Part I. Experimental study of the nitrogen–oxygen–carbon dioxide system at 0°C," *AIChE J.*, vool. 11 (6), pp. 1092–1096, 1965, doi: 10.1002/aic.690110624.

[42] I. Al-Siyabi, "Effect of impurities on CO_2 streams," no. February, 2013, PhD Thesis, Heriot-Watt University, Edinburgh 2013.

[43] R. Klimeck, "Entwicklung einer Fundamentalgleichung für Erdgase für das Gas- und Flüssigkeitsgebiet sowie das Phasengleichgewicht," Doctoral Thesis, Ruhr-Universität Bochum, Bochum, Germany, 2000.

[44] R. Span and W. Wagner, "Equations of State for Technical Applications. II. Results for Nonpolar Fluids," *International Journal of Thermophysics*. vol. 24, pp. 41–109, 2003, doi: 10.1023/A:1022310214958.

[45] M. Mazzoccoli, B. Bosio, and E. Arato, "Pressure–density–temperature measurements of binary mixtures rich in CO_2 for pipeline transportation in the CCS process," *J. Chem. Eng. Data*, vol. 57 (10), pp. 2774–2783, 2012, doi: 10.1021/je300590v.

[46] G. J. Gururaja, M. A. Tirunarayanan, and A. Ramachandran, "Dynamic Viscosity of Gas Mixtures," *J. Chem. Eng. Data*, vol. 12, no. 4, pp. 562–567, 1967, doi: 10.1021/je60035a024.

[47] S. F. Westman, H. G. J. Stang, S. W. Løvseth, A. Austegard, I. Snustad, and I. S. Ertesvåg, "Vapor-liquid equilibrium data for the carbon dioxide and oxygen (CO_2 + O_2) system at the

temperatures 218, 233, 253, 273, 288 and 298 K and pressures up to 14 MPa," *Fluid Phase Equilib.*, vol. 421, pp. 67–87, 2016, doi: 10.1016/j.fluid.2016.04.002.

[48] M. Ahmad, J. Gernert, and E. Wilbers, "Effect of impurities in captured CO2 on liquid-vapor equilibrium," *Fluid Phase Equilib.*, 2014, doi: 10.1016/j.fluid.2013.11.009.

[49] A. Fredenslund, J. Mollerup, and O. Persson, "Gas-Liquid Equilibrium of Oxygen-Carbon Dioxide System," *J. Chem. Eng. Data*, vol. 17, no. 4, pp. 440–443, 1972, doi: 10.1021/je60055a019.

[50] H. S. Booth and J. M. Carter, "The critical constants of carbon dioxide-oxygen mixtures," *J. Phys. Chem.*, vol. 34, no. 12, pp. 2801–2825, 1930, doi: 10.1021/j150318a013.

[51] P. H. van Konynenburg and R. L. Scott, "Critical lines and phase equilibria in binary van der Waals mixtures," *Philos. Trans. R. Soc. London. Ser. A, Math. Phys. Sci.*, vol. 298, pp. 495–540, 1980, doi: 10.1098/rsta.1980.0266.

[52] R. Privat and J. N. Jaubert, "Classification of global fluid-phase equilibrium behaviors in binary systems," *Chem. Eng. Res. Des.*, vol. 91 (10), pp. 1807–1839, 2013, doi: 10.1016/j.cherd.2013.06.026.

[53] J.A. Commodore, C.E. Deering, R.A. Marriott, "Volumetric properties and phase behavior of sulfur dioxide, carbon disulfide and oxygen in high-pressure carbon dioxide fluid". *Fluid Phase Equilib*. 2018; 477:30-39. https://doi.org/10.1016/j.fluid.2018.08.012

[54] Muirbrook NK. Experimental and thermodynamic study of the high-pressure vapor-liquid equilibria for the nitrogen-oxygen-carbon dioxide system. Ph.D. Thesis, University of California, Berkeley 1964.

Figures

Figure 1. *p*, *T*-phase diagram showing the experimental points measured (●) and the calculated phase envelope (solid line) using the EOS-CG [3] for: (a) (0.50 CO_2 + 0.50 O_2) and (b) (0.25 CO_2 + 0.75 O_2) binary mixtures, respectively. The marked temperature and pressure ranges represent the range of the binary experimental data used for the development of the EOS-CG (red dashed line), the GERG-2008 EoS (blue dashed line), and the area of interest for the gas industry (black thin dashed line).

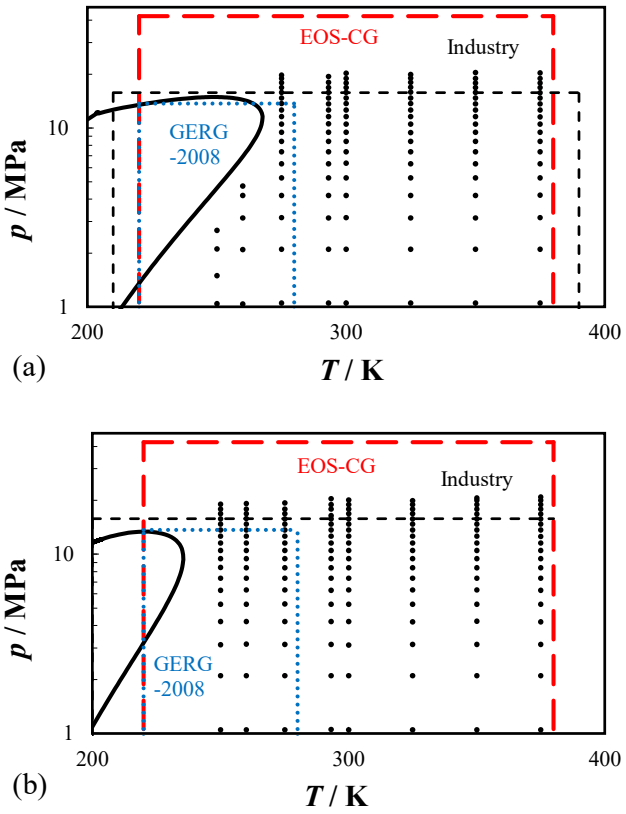

Figure 2. Relative deviations in density of the experimental (p,ρ_{exp},T) data of the binary (0.50 CO_2 + 0.50 O_2) mixture from density values calculated by the: (a) GERG-2008 [2], ρ_{GERG}, and (b) EOS-CG [3], ρ_{CG}, equations of state as a function of pressure for different temperatures: ◇ 250 K, △ 260 K, × 275 K, □ 293.15 K, ○ 300 K, + 325 K, ✳ 350 K, — 375 K. Dashed lines indicate the expanded (k = 2) uncertainty of the corresponding EoS. Error bars on the 293.15 K data set indicate the expanded (k = 2) uncertainty of the experimental density.

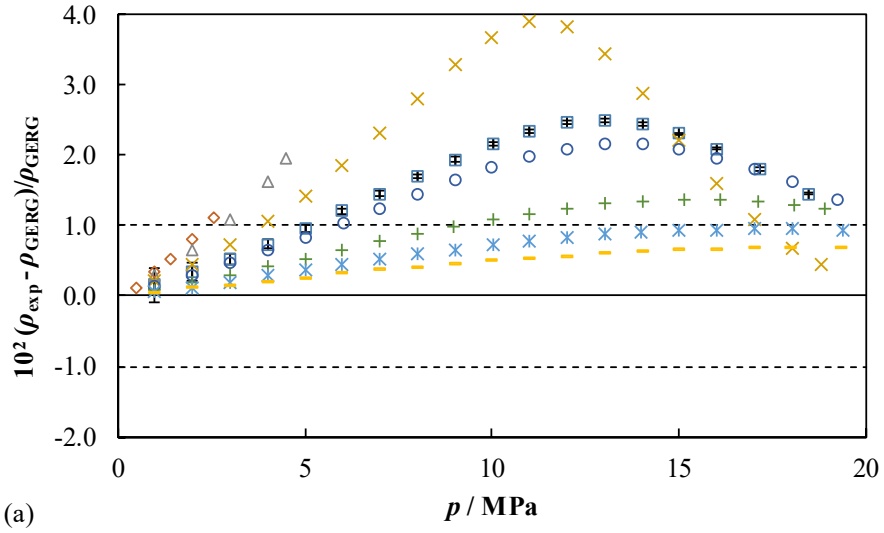

(a)

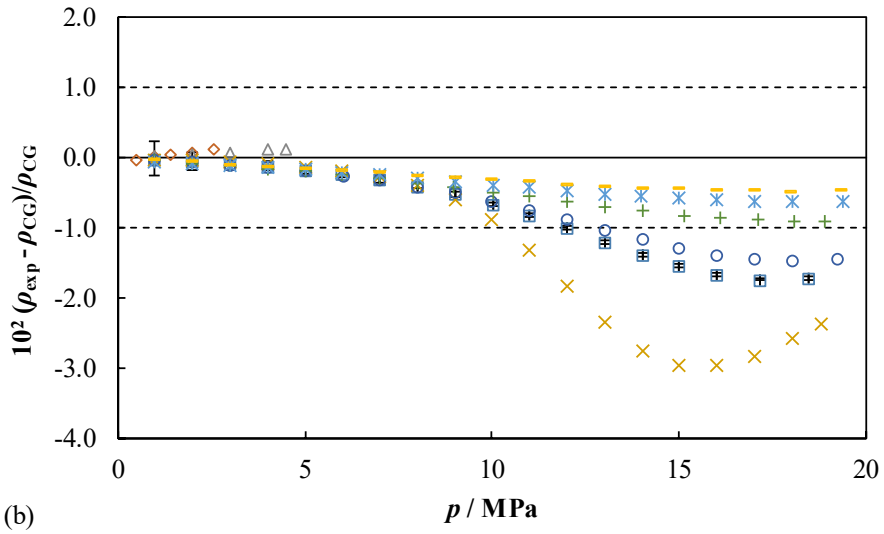

(b)

Figure 3. Relative deviations in density of the experimental (p,ρ_{exp},T) data of the binary (0.25 CO_2 + 0.75 O_2) mixture from density values calculated by the: (a) GERG-2008 [2], ρ_{GERG}, and (b) EOS-CG [3], ρ_{CG}, equations of state as a function of pressure for different temperatures: ◇ 250 K, △ 260 K, × 275 K, □ 293.15 K, ○ 300 K, + 325 K, ✳ 350 K, — 375 K. Dashed lines indicate the expanded (k = 2) uncertainty of the corresponding EoS. Error bars on the 293.15 K data set indicate the expanded (k = 2) uncertainty of the experimental density.

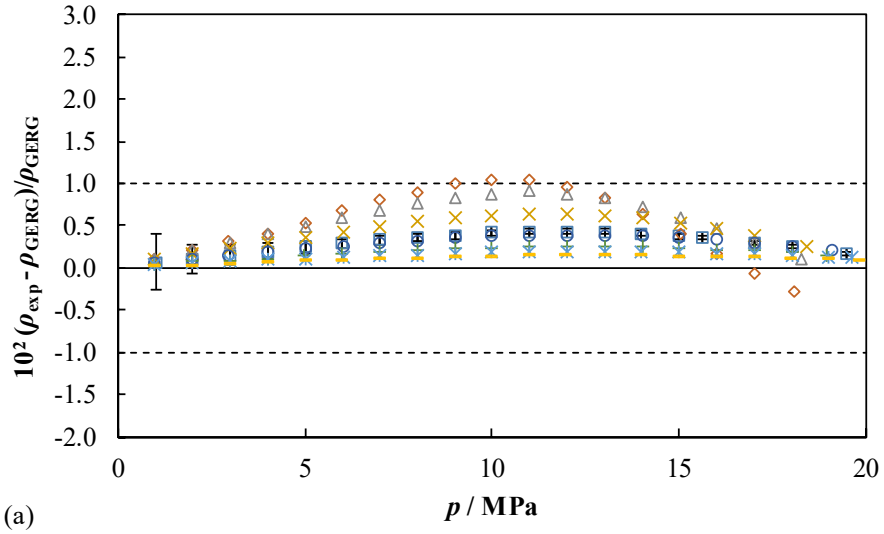

(a)

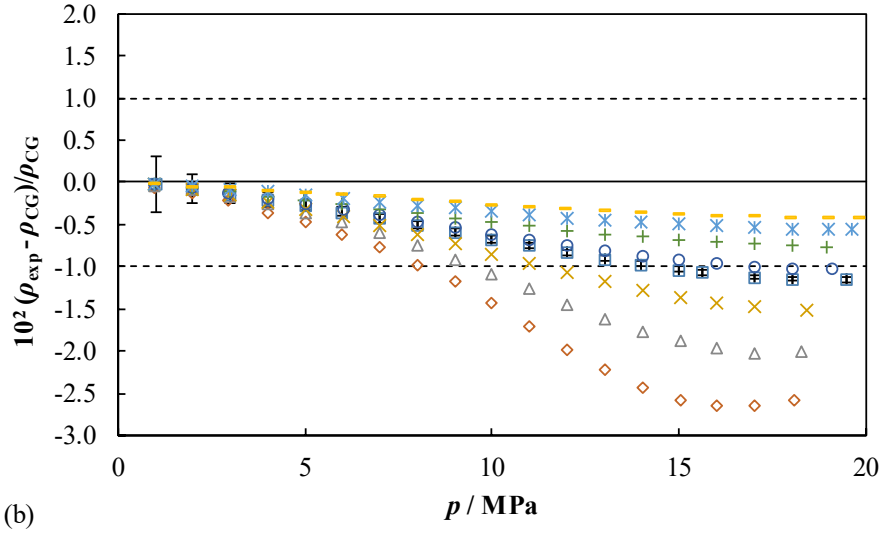

(b)

Figure 4. Second interaction virial coefficient $B_{12}(T)$ for the binary (CO_2 + O_2) system estimated from the experimental data as a function of the O_2 mole fraction, $x(O_2)$, at different temperatures: ◇ 250 K, Δ 260 K, × 275 K, ○ 300 K, + 325 K, ✳ 350 K, − 375 K. The dashed lines represent the $B_{12}(T)$ values computed from the EOS-CG at the corresponding temperatures.

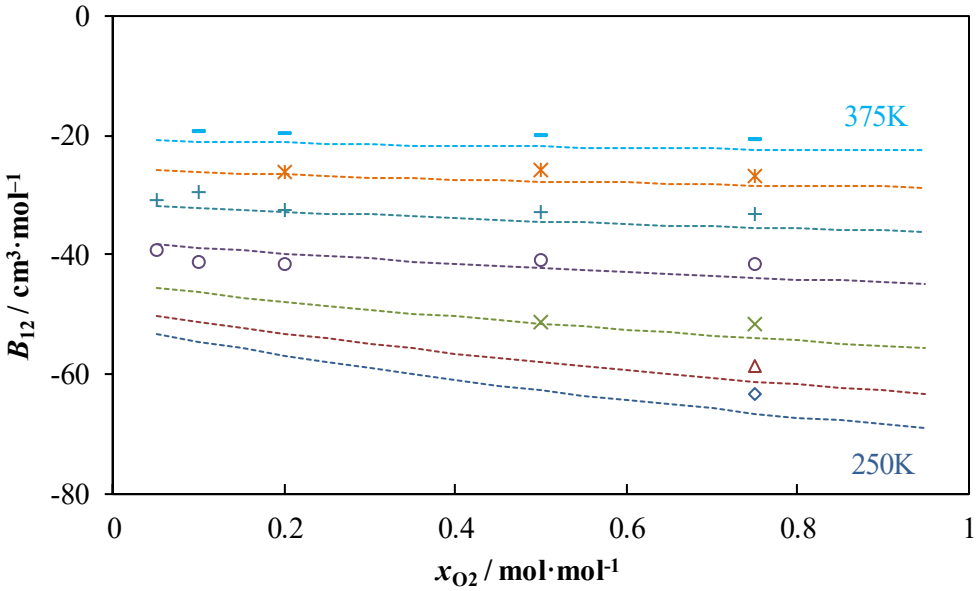

Figure 5. (a) Mean value of the second interaction virial coefficient $B_{12}(T)$ for the binary (CO_2 + O_2) system as a function of temperature from: × this work, Δ Martin et al. [35], ◇ Edwards and Roseveare [37], □ Gorski and Miller [36], ○ Cottrell et al. [38], - - GERG-2008 EoS [2], ··· EOS-CG [3]. Error bars indicate the expanded (k = 2) uncertainty of the estimated $B_{12}(T)$ values. The solid line represents the fit to equation (8) of the experimental data of this work. (b) Residuals of the fit to equation (8).

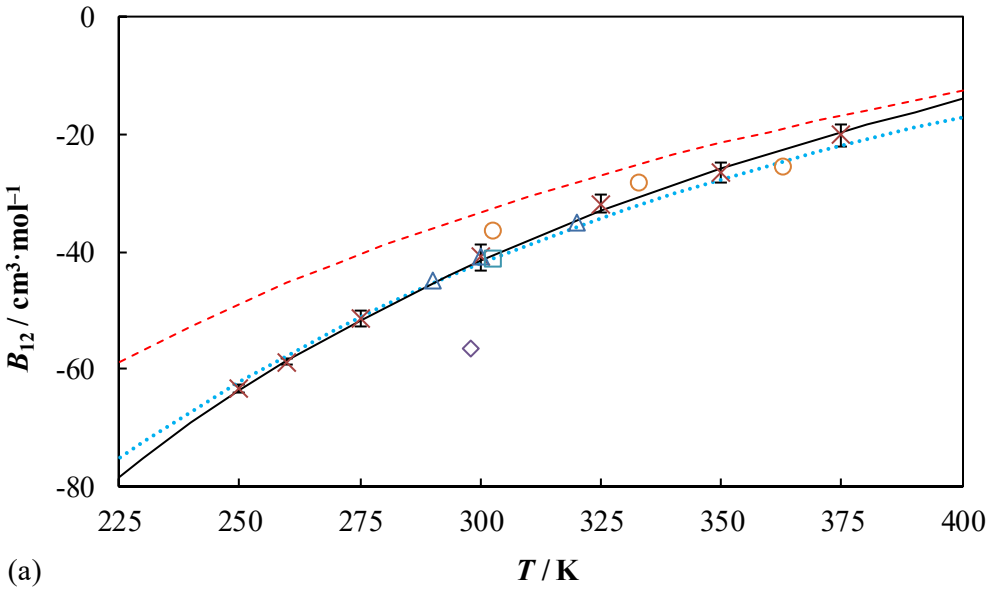

(a)

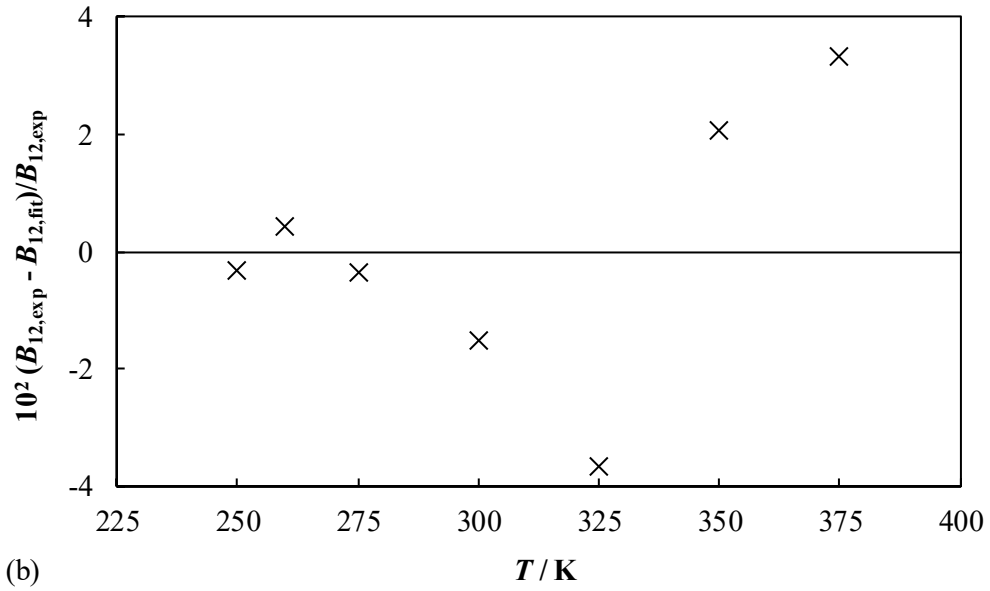

(b)

Figure 6. Relative deviations in (density or pressure) of the experimental (p_{exp}, ρ_{exp}, T) data of the five binary (CO_2 + O_2) mixtures measured in this work and in part one of this study [1], from (density or pressure) values calculated by the: (a) GERG-2008 [2], ρ_{GERG}, (b) EOS-CG [3], ρ_{CG}, and (c) virial equation of state, p_{virial}, as a function of density for different oxygen contents: ○ $x(O_2) = 0.05$, × $x(O_2) = 0.10$, △ $x(O_2) = 0.20$, ◇ $x(O_2) = 0.50$, and □ $x(O_2) = 0.75$. Dashed lines indicate the expanded ($k = 2$) uncertainty of the corresponding EoS (1 % threshold).

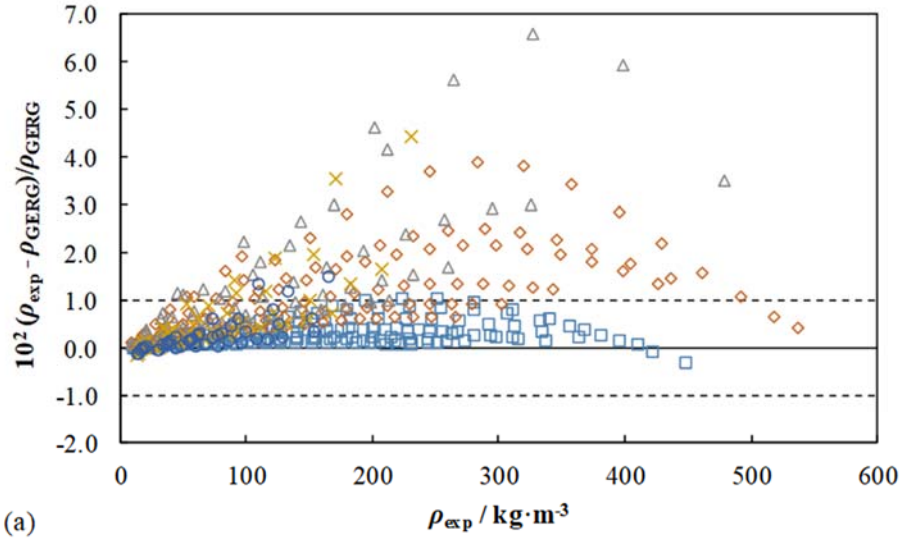
7.0
6.0
5.0
4.0
3.0
2.0
1.0
0.0
-1.0
-2.0
0
100
200
300
400
500
600
$10^2\,(\rho_{exp} - \rho_{GERG})/\rho_{GERG}$
ρ_{exp} / kg·m^{-3}

(a)

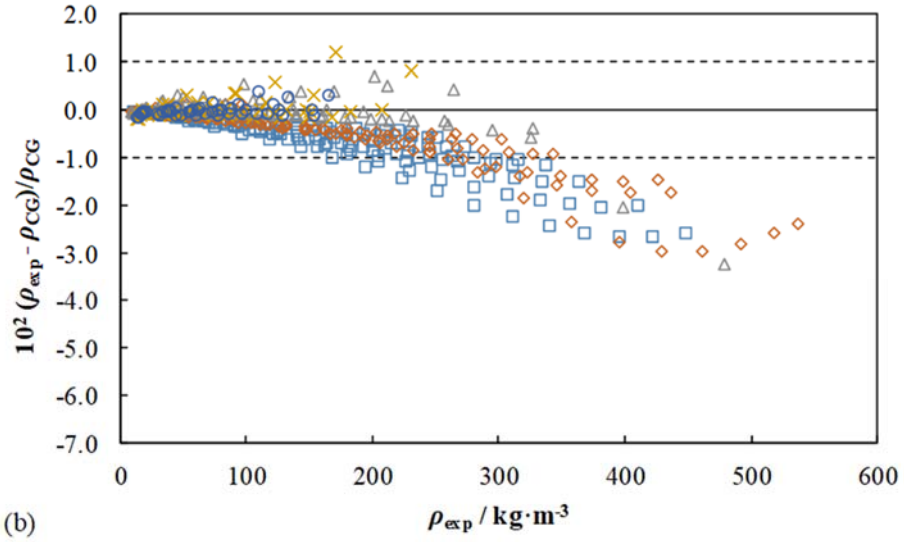
2.0
1.0
0.0
-1.0
-2.0
-3.0
-4.0
-5.0
-6.0
-7.0
0
100
200
300
400
500
600
$10^2\,(\rho_{exp} - \rho_{CG})/\rho_{CG}$
ρ_{exp} / kg·m^{-3}

(b)

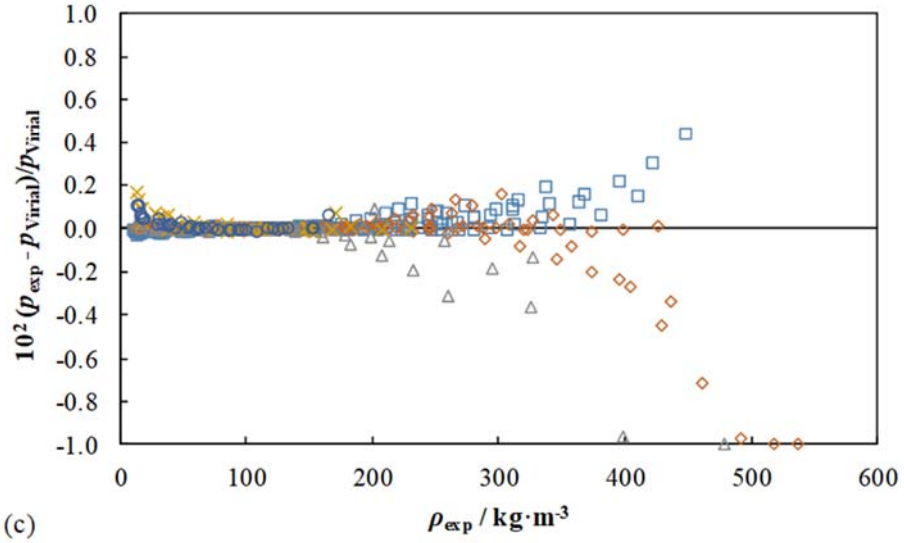
1.0
0.8
0.6
0.4
0.2
0.0
-0.2
-0.4
-0.6
-0.8
-1.0
0
100
200
300
400
500
600
$10^2\,(p_{exp} - p_{Virial})/p_{Virial}$
ρ_{exp} / kg·m^{-3}

(c)

Tables

Table 1. Purity, supplier, molar mass, and critical parameters for the constituting components of the studied (CO_2 + O_2) mixtures in this work.

	Purity / vol-%	Supplier	M / g·mol^{-1}	Critical parameters[a]	
				T_c / K	p_c / MPa
Carbon dioxide	99.9995	Air Liquide	44.010	304.13	7.3773
Oxygen	99.9999	Linde	31.999	154.58	5.0430

[a] Critical parameters were obtained by using the default equation for each substance in REFPROP software [29].

Table 2. Composition of the studied binary (CO_2 + O_2) mixtures in this work. Impurity compounds are marked in *italic* type.

Component	(0.50 CO_2 + 0.50 O_2)[a]		(0.25 CO_2 + 0.75 O_2)[b]	
	$10^2\ x_i$ / mol/mol	$10^2\ U(x_i)$ / mol/mol	$10^2\ x_i$ / mol/mol	$10^2\ U(x_i)$ / mol/mol
Carbon dioxide	50.002657	0.000565	25.008606	0.000563
Oxygen	49.997192	0.000781	74.991234	0.000788
Argon	0.000050	0.000058	0.000075	0.000087
Nitrogen	0.000075	0.000065	0.000063	0.000052
Carbon monoxide	0.000020	0.000018	0.000015	0.000012
Propane	0.000004	0.000004	0.000005	0.000006
Nitric oxide	0.000002	0.000003	0.000001	0.000001
Normalized composition without impurities				
Carbon dioxide	50.002733	0.000565	25.008646	0.000563
Oxygen	49.997267	0.000781	74.991354	0.000788

[a] BAM cylinder no.: 1009-180717

[b] BAM cylinder no.: 1099-180717

Table 3. Results of the gas chromatographic (GC) analysis and relative deviations between gravimetric preparation and GC analysis for the three (CO_2 + O_2) mixtures studied in this work. The results are followed by the gravimetric composition (non-normalized) of the employed validation mixtures.

Component	Concentration		Relative deviation between gravimetric composition and GC analysis
	$10^2\ x_i$ / mol/mol	$10^2\ U(x_i)$ / mol/mol	%
(0.50 CO_2 + 0.50 O_2) BAM cylinder no.: 1009-180717			
Carbon dioxide	49.9663	0.0539	−0.073
Oxygen	n. a.	n. a.	—
Validation mixture BAM cylinder no.: 96055001-980401 (G 050)			
Carbon dioxide	49.906395	0.000918	
Nitrogen	50.093282	0.001397	
Oxygen	0.000240	0.000271	
Carbon monoxide	0.000077	0.000087	
Hydrogen	0.000006	0.000007	
Validation mixture BAM cylinder no.: 8063-141006 (premixture G 473)			
Carbon dioxide	51.479531	0.000953	
Nitrogen	44.109490	0.001903	
Oxygen	4.410942	0.000341	
Argon	0.000009	0.000010	
Carbon monoxide	0.000019	0.000018	
Methane	0.000001	0.000001	
Hydrogen	0.000007	0.000006	
Nitric oxide	0.000002	0.000003	
(0.25 CO_2 + 0.75 O_2) BAM cylinder no.: 1099-180717			
Carbon dioxide	24.9755	0.0377	−0.132

Oxygen	n. a.	n. a.	—
Validation mixture BAM cylinder no.: C49312-010509 (G 050)			
Carbon dioxide	25.020915	0.000536	
Nitrogen	74.979048	0.000842	
Oxygen	0.000016	0.000013	
Carbon monoxide	0.000011	0.000010	
Hydrogen	0.000009	0.000011	
Nitric oxide	0.000001	0.000001	
Validation mixture BAM cylinder no.: 5018-020710 (G 050)			
Carbon dioxide	27.264804	0.000521	
Nitrogen	72.735158	0.000819	
Oxygen	0.000016	0.000013	
Carbon monoxide	0.000012	0.000010	
Hydrogen	0.000009	0.000011	
Nitric oxide	0.000001	0.000002	

Table 4. Contributions to the expanded ($k = 2$) overall uncertainty in density, $U_T(\rho_{exp})$, for the two (CO_2 + O_2) mixtures studied in this work.

Source	Contribution ($k = 2$)	Units	Estimation in density ($k = 2$)	
			$kg \cdot m^{-3}$	%
		(0.50 CO_2 + 0.50 O_2)		
Temperature, T	0.004	K	< 0.025	< 0.0061
Pressure, p	< 0.005	MPa	(0.045 – 0.18)	(0.021 – 0.73)
Composition, x_i	< 0.0004	$mol \cdot mol^{-1}$	< 0.010	< 0.0022
Density, ρ	(0.036 – 0.099)	$kg \cdot m^{-3}$	(0.036 – 0.099)	(0.019 – 0.44)
Sum			(0.057 – 0.20)	(0.028 – 0.85)
		(0.25 CO_2 + 0.75 O_2)		
Temperature, T	0.004	K	< 0.020	< 0.0048
Pressure, p	< 0.005	MPa	(0.041 – 0.14)	(0.025 – 0.37)
Composition, x_i	< 0.0004	$mol \cdot mol^{-1}$	< 0.073	< 0.0017
Density, ρ	(0.042 – 0.101)	$kg \cdot m^{-3}$	(0.042 – 0.10)	(0.023 – 0.38)
Sum			(0.059 – 0.17)	(0.035 – 0.52)

Table 5. Experimental (p, ρ_{exp}, T) measurements for the binary (0.50 CO_2 + 0.50 O_2) mixture, absolute and relative expanded (k = 2) uncertainty in density, $U(\rho_{exp})$, and relative deviations from the density given by the GERG-2008 [2], ρ_{GERG}, and the EOS-CG [3], ρ_{CG}, equations of state.

T / K[(a)]	p / MPa[(a)]	ρ_{exp} / kg·m^{-3}	$U(\rho_{exp})$ / kg·m^{-3}	10^2 $U(\rho_{exp})/\rho_{exp}$	10^2 (ρ_{exp} - ρ_{GERG})/ρ_{GERG}	10^2 (ρ_{exp} - ρ_{CG})/ρ_{CG}
			250 K isotherm			
250.046	2.551	52.505	0.046	0.087	1.10	0.12
250.047	2.006	40.148	0.044	0.110	0.81	0.08
250.044	1.420	27.631	0.043	0.155	0.53	0.05
250.045	0.994	18.956	0.042	0.221	0.34	0.02
250.044	0.498	9.294	0.041	0.438	0.12	-0.03
			260 K isotherm			
260.047	4.511	96.518	0.050	0.052	1.95	0.13
260.046	4.000	83.332	0.049	0.058	1.63	0.11
260.046	2.988	59.290	0.046	0.077	1.09	0.07
260.041	1.989	37.763	0.043	0.115	0.65	0.04
260.044	0.986	17.990	0.041	0.228	0.30	0.02
			275 K isotherm			
275.018	18.783	536.868	0.099	0.019	0.44	-2.36
275.016	18.027	518.230	0.097	0.019	0.68	-2.57
275.014	17.023	491.321	0.094	0.019	1.08	-2.81
275.012	16.026	461.967	0.091	0.020	1.59	-2.95
275.012	15.013	429.453	0.087	0.020	2.22	-2.94
275.010	14.020	395.120	0.083	0.021	2.87	-2.74
275.008	13.018	358.480	0.079	0.022	3.45	-2.34
275.008	12.009	320.447	0.075	0.023	3.82	-1.83
275.007	11.009	282.804	0.070	0.025	3.90	-1.31

275.005	10.006	246.161	0.066	0.027	3.69	-0.89
275.003	9.005	211.687	0.062	0.029	3.29	-0.59
275.004	8.005	179.703	0.059	0.033	2.81	-0.39
275.003	7.002	150.278	0.055	0.037	2.32	-0.26
275.003	6.001	123.367	0.052	0.042	1.85	-0.18
275.003	5.000	98.668	0.049	0.050	1.43	-0.13
275.002	3.999	75.936	0.047	0.062	1.06	-0.09
275.001	3.004	55.017	0.044	0.081	0.74	-0.06
275.001	1.999	35.366	0.042	0.119	0.45	-0.04
275.002	0.999	17.108	0.040	0.234	0.21	-0.02
			293.15 K isotherm			
293.091	18.436	436.376	0.087	0.020	1.46	-1.72
293.092	17.141	403.789	0.083	0.021	1.80	-1.73
293.093	16.006	373.566	0.080	0.021	2.10	-1.66
293.093	15.005	345.809	0.077	0.022	2.30	-1.55
293.094	14.010	317.600	0.073	0.023	2.44	-1.39
293.093	13.006	288.886	0.070	0.024	2.50	-1.20
293.094	12.007	260.508	0.067	0.026	2.46	-1.01
293.094	11.007	232.662	0.064	0.027	2.35	-0.82
293.092	10.043	206.648	0.061	0.029	2.17	-0.67
293.092	9.011	179.946	0.058	0.032	1.94	-0.53
293.094	8.003	155.119	0.055	0.035	1.70	-0.41
293.092	7.001	131.760	0.052	0.040	1.46	-0.31
293.092	6.009	109.848	0.050	0.045	1.21	-0.24
293.092	5.000	88.810	0.047	0.053	0.96	-0.18
293.093	3.999	69.090	0.045	0.065	0.74	-0.13
293.092	2.985	50.178	0.043	0.086	0.52	-0.09

293.092	1.999	32.751	0.041	0.125	0.34	-0.05
293.092	0.999	15.954	0.039	0.245	0.16	-0.02
			300 K isotherm			
299.947	19.218	426.654	0.086	0.020	1.38	-1.44
299.946	18.017	398.813	0.082	0.021	1.62	-1.47
299.947	17.009	374.312	0.080	0.021	1.81	-1.44
299.946	16.013	349.239	0.077	0.022	1.97	-1.38
299.944	15.010	323.405	0.074	0.023	2.09	-1.28
299.947	14.010	297.246	0.071	0.024	2.16	-1.16
299.945	13.010	271.079	0.068	0.025	2.16	-1.02
299.947	12.006	245.004	0.065	0.026	2.10	-0.88
299.945	11.006	219.591	0.062	0.028	1.99	-0.74
299.946	10.005	194.857	0.059	0.030	1.83	-0.61
299.945	9.004	171.008	0.056	0.033	1.65	-0.50
299.947	8.002	148.143	0.054	0.036	1.45	-0.41
299.948	7.002	126.328	0.051	0.041	1.25	-0.32
299.946	6.038	106.284	0.049	0.046	1.05	-0.25
299.947	5.008	85.884	0.047	0.054	0.84	-0.19
299.945	4.001	66.926	0.045	0.067	0.65	-0.13
299.945	3.000	48.979	0.042	0.087	0.47	-0.09
299.946	1.999	31.881	0.041	0.127	0.31	-0.05
299.946	0.999	15.565	0.039	0.249	0.15	-0.03
			325 K isotherm			
324.952	18.906	343.259	0.075	0.022	1.25	-0.91
324.952	18.076	327.073	0.073	0.022	1.30	-0.90
324.953	17.106	307.850	0.071	0.023	1.34	-0.89
324.952	16.105	287.748	0.069	0.024	1.36	-0.85

324.952	15.122	267.889	0.066	0.025	1.37	-0.81
324.953	14.008	245.322	0.064	0.026	1.35	-0.75
324.952	13.013	225.252	0.062	0.027	1.31	-0.69
324.953	11.990	204.805	0.059	0.029	1.25	-0.63
324.953	11.012	185.551	0.057	0.031	1.18	-0.55
324.953	10.011	166.210	0.055	0.033	1.09	-0.49
324.952	8.969	146.502	0.053	0.036	0.98	-0.42
324.953	8.001	128.664	0.051	0.039	0.88	-0.36
324.953	7.004	110.806	0.048	0.044	0.77	-0.29
324.953	6.002	93.365	0.046	0.050	0.65	-0.24
324.953	5.001	76.501	0.045	0.058	0.54	-0.19
324.951	3.999	60.141	0.043	0.071	0.42	-0.15
324.951	2.986	44.141	0.041	0.093	0.31	-0.11
324.951	2.000	29.078	0.039	0.135	0.20	-0.07
324.951	0.999	14.286	0.037	0.262	0.09	-0.04
			350 K isotherm			
349.935	19.393	302.011	0.069	0.023	0.93	-0.62
349.936	18.003	279.264	0.067	0.024	0.95	-0.62
349.935	17.004	262.723	0.065	0.025	0.95	-0.61
349.935	16.001	246.017	0.063	0.026	0.95	-0.59
349.935	15.004	229.333	0.061	0.027	0.93	-0.57
349.934	14.003	212.603	0.059	0.028	0.91	-0.54
349.934	13.000	195.872	0.057	0.029	0.87	-0.51
349.935	12.001	179.322	0.055	0.031	0.83	-0.47
349.935	11.001	162.916	0.054	0.033	0.78	-0.42
349.934	10.021	147.007	0.052	0.035	0.72	-0.38
349.936	9.000	130.648	0.050	0.038	0.66	-0.34

349.935	8.000	114.907	0.048	0.042	0.59	-0.29
349.935	7.000	99.435	0.046	0.047	0.52	-0.25
349.935	6.000	84.254	0.045	0.053	0.45	-0.21
349.935	5.000	69.392	0.043	0.062	0.37	-0.17
349.936	3.999	54.846	0.041	0.075	0.29	-0.13
349.936	2.985	40.432	0.040	0.098	0.20	-0.11
349.935	1.999	26.749	0.038	0.142	0.12	-0.08
349.935	1.000	13.220	0.036	0.276	0.05	-0.05
			375 K isotherm			
374.922	19.304	265.337	0.064	0.024	0.67	-0.48
374.922	18.002	246.901	0.062	0.025	0.67	-0.48
374.922	16.998	232.559	0.061	0.026	0.67	-0.48
374.921	15.996	218.186	0.059	0.027	0.66	-0.47
374.920	14.998	203.822	0.057	0.028	0.64	-0.45
374.921	14.017	189.691	0.056	0.029	0.62	-0.43
374.921	12.998	175.041	0.054	0.031	0.59	-0.41
374.920	11.999	160.727	0.052	0.033	0.56	-0.38
374.920	10.999	146.474	0.051	0.035	0.53	-0.35
374.919	10.000	132.318	0.049	0.037	0.49	-0.32
374.921	9.000	118.279	0.048	0.040	0.45	-0.29
374.920	7.999	104.368	0.046	0.044	0.40	-0.25
374.921	6.999	90.633	0.044	0.049	0.36	-0.21
374.922	6.000	77.083	0.043	0.056	0.31	-0.18
374.920	5.000	63.711	0.041	0.065	0.25	-0.15
374.920	4.005	50.603	0.040	0.079	0.20	-0.12
374.921	2.998	37.555	0.038	0.102	0.15	-0.10
374.922	2.000	24.835	0.037	0.149	0.10	-0.06

374.921	0.999	12.288	0.036	0.289	0.05	-0.03

[(a)] Expanded uncertainties ($k = 2$): $U(p > 3)/\text{MPa} = 75 \cdot 10^{-6} \cdot \frac{p}{\text{MPa}} + 3.5 \cdot 10^{-3}$; $U(p < 3)/\text{MPa} = 60 \cdot 10^{-6} \cdot \frac{p}{\text{MPa}} + 1.7 \cdot 10^{-3}$; $U(T) = 4$ mK; $\frac{U(\rho)}{\text{kg·m}^{-3}} = 2.5 \cdot 10^{4} \frac{\chi_S}{\text{m}^3\cdot\text{kg}^{-1}} + 1.1 \cdot 10^{-4} \cdot \frac{\rho}{\text{kg·m}^{-3}} + 2.3 \cdot 10^{-2}$.

Table 6. Experimental (p, ρ_{exp}, T) measurements for the binary (0.25 CO_2 + 0.75 O_2) mixture, absolute and relative expanded (k = 2) uncertainty in density, $U(\rho_{exp})$, and relative deviations from the density given by the GERG-2008 [2], ρ_{GERG}, and the EOS-CG [3], ρ_{CG}, equations of state.

T / K[(a)]	p / MPa[(a)]	ρ_{exp} / kg·m^{-3}[(a)]	$U(\rho_{exp})$ / kg·m^{-3}	10^2 $U(\rho_{exp})/\rho_{exp}$	10^2 (ρ_{exp} - ρ_{GERG})/ρ_{GERG}	10^2 (ρ_{exp} - ρ_{CG})/ρ_{CG}
250 K isotherm						
250.033	18.094	448.577	0.101	0.023	-0.28	-2.57
250.034	17.025	422.254	0.098	0.023	-0.06	-2.64
250.031	16.013	395.828	0.095	0.024	0.17	-2.64
250.034	15.018	368.491	0.092	0.025	0.41	-2.56
250.035	14.016	339.912	0.089	0.026	0.63	-2.42
250.035	13.015	310.671	0.086	0.028	0.82	-2.22
250.034	12.010	281.022	0.082	0.029	0.96	-1.97
250.032	11.005	251.582	0.079	0.031	1.04	-1.69
250.033	10.007	222.915	0.076	0.034	1.05	-1.42
250.032	9.005	195.078	0.072	0.037	1.00	-1.17
250.021	8.017	168.747	0.069	0.041	0.90	-0.97
250.015	7.001	143.020	0.066	0.046	0.80	-0.77
250.012	6.002	119.016	0.064	0.054	0.67	-0.61
250.013	5.000	96.291	0.061	0.063	0.54	-0.47
250.012	3.999	74.849	0.059	0.078	0.41	-0.35
250.021	2.975	54.134	0.056	0.104	0.32	-0.21
250.031	1.999	35.419	0.054	0.153	0.21	-0.12
250.029	0.999	17.245	0.052	0.302	0.11	-0.05
260 K isotherm						
260.029	18.272	410.337	0.096	0.023	0.10	-2.00
260.030	17.019	381.362	0.093	0.024	0.30	-2.01

260.029	16.011	357.028	0.090	0.025	0.46	-1.96
260.028	15.031	332.575	0.087	0.026	0.60	-1.88
260.028	14.021	306.829	0.084	0.027	0.73	-1.76
260.026	13.011	280.775	0.081	0.029	0.82	-1.61
260.025	12.009	254.904	0.078	0.031	0.88	-1.44
260.027	11.006	229.285	0.075	0.033	0.91	-1.25
260.027	10.003	204.098	0.072	0.035	0.88	-1.07
260.025	9.003	179.682	0.070	0.039	0.84	-0.90
260.027	8.005	156.109	0.067	0.043	0.76	-0.75
260.026	7.006	133.454	0.064	0.048	0.68	-0.60
260.025	6.005	111.681	0.062	0.055	0.59	-0.46
260.025	5.013	91.047	0.059	0.065	0.50	-0.35
260.026	4.001	70.943	0.057	0.081	0.40	-0.25
260.023	3.000	51.968	0.055	0.106	0.30	-0.16
260.024	2.000	33.855	0.053	0.156	0.21	-0.08
260.024	0.999	16.536	0.051	0.308	0.11	-0.02
			275 K isotherm			
274.994	18.413	363.002	0.089	0.025	0.25	-1.50
274.992	17.016	334.214	0.086	0.026	0.38	-1.47
274.996	16.006	312.797	0.083	0.027	0.46	-1.42
274.998	15.022	291.571	0.081	0.028	0.53	-1.36
274.997	14.008	269.483	0.078	0.029	0.59	-1.27
274.998	13.009	247.616	0.076	0.031	0.63	-1.17
274.998	12.008	225.785	0.073	0.033	0.64	-1.07
274.998	11.003	204.069	0.071	0.035	0.65	-0.95
274.998	10.004	182.777	0.068	0.037	0.62	-0.83
274.998	9.002	161.854	0.066	0.041	0.59	-0.72

274.997	8.002	141.471	0.064	0.045	0.54	-0.61
274.997	7.010	121.823	0.062	0.051	0.49	-0.50
274.996	6.013	102.658	0.059	0.058	0.43	-0.40
274.996	5.032	84.400	0.057	0.068	0.37	-0.31
274.996	4.005	65.923	0.055	0.084	0.30	-0.22
274.995	2.995	48.398	0.053	0.110	0.23	-0.14
274.995	1.999	31.732	0.051	0.162	0.16	-0.07
274.996	0.999	15.571	0.049	0.317	0.10	-0.01
			293.15 K isotherm			
293.086	19.488	337.017	0.085	0.025	0.17	-1.15
293.082	18.016	311.066	0.082	0.026	0.25	-1.14
293.079	17.009	292.913	0.080	0.027	0.30	-1.12
293.079	15.615	267.384	0.077	0.029	0.36	-1.06
293.078	15.008	256.154	0.075	0.029	0.38	-1.03
293.082	13.998	237.416	0.073	0.031	0.41	-0.97
293.085	13.004	218.912	0.071	0.032	0.42	-0.90
293.088	12.006	200.401	0.069	0.034	0.43	-0.83
293.088	11.004	181.957	0.067	0.037	0.43	-0.75
293.088	10.004	163.705	0.065	0.040	0.41	-0.67
293.089	9.002	145.672	0.063	0.043	0.39	-0.59
293.089	8.002	127.961	0.061	0.047	0.36	-0.50
293.089	7.001	110.579	0.059	0.053	0.33	-0.42
293.090	6.001	93.576	0.057	0.061	0.29	-0.34
293.088	5.000	76.953	0.055	0.071	0.24	-0.27
293.088	3.999	60.720	0.053	0.087	0.20	-0.20
293.089	2.992	44.801	0.051	0.114	0.15	-0.13
293.089	2.001	29.567	0.050	0.167	0.11	-0.07

293.090	1.002	14.596	0.048	0.328	0.07	-0.02
			300 K isotherm			
299.942	19.099	316.114	0.082	0.026	0.21	-1.02
299.942	18.014	297.775	0.080	0.027	0.26	-1.01
299.942	17.010	280.533	0.078	0.028	0.30	-0.99
299.944	16.011	263.168	0.076	0.029	0.33	-0.96
299.942	15.009	245.604	0.074	0.030	0.36	-0.92
299.943	14.009	227.985	0.072	0.031	0.38	-0.87
299.943	13.007	210.309	0.070	0.033	0.39	-0.81
299.944	12.005	192.673	0.068	0.035	0.39	-0.75
299.944	11.004	175.153	0.066	0.037	0.39	-0.67
299.942	10.004	157.797	0.064	0.040	0.37	-0.60
299.942	9.002	140.615	0.062	0.044	0.35	-0.53
299.941	8.013	123.873	0.060	0.048	0.33	-0.46
299.942	7.006	107.131	0.058	0.054	0.30	-0.38
299.941	6.023	91.070	0.056	0.061	0.26	-0.31
299.943	5.002	74.728	0.054	0.072	0.22	-0.24
299.942	4.001	59.065	0.052	0.089	0.18	-0.18
299.942	2.963	43.181	0.051	0.117	0.14	-0.12
299.941	1.999	28.786	0.049	0.170	0.11	-0.06
299.944	0.999	14.204	0.047	0.333	0.07	-0.01
			325 K isotherm			
324.952	18.940	272.696	0.075	0.027	0.16	-0.75
324.952	18.004	259.112	0.073	0.028	0.18	-0.74
324.952	17.018	244.643	0.072	0.029	0.20	-0.73
324.952	16.007	229.703	0.070	0.031	0.22	-0.70
324.953	15.007	214.817	0.068	0.032	0.23	-0.67

324.952	14.007	199.880	0.067	0.033	0.24	-0.64
324.952	13.004	184.876	0.065	0.035	0.25	-0.60
324.952	12.002	169.876	0.063	0.037	0.25	-0.56
324.952	11.002	154.959	0.062	0.040	0.25	-0.51
324.951	10.002	140.094	0.060	0.043	0.24	-0.46
324.951	9.002	125.321	0.058	0.046	0.22	-0.41
324.951	8.001	110.662	0.057	0.051	0.21	-0.36
324.952	7.008	96.262	0.055	0.057	0.19	-0.30
324.951	6.005	81.875	0.053	0.065	0.17	-0.25
324.953	4.998	67.607	0.052	0.076	0.14	-0.20
324.952	3.993	53.574	0.050	0.093	0.11	-0.15
324.952	2.991	39.794	0.048	0.122	0.09	-0.10
324.952	2.001	26.394	0.047	0.178	0.07	-0.05
324.954	0.995	13.010	0.045	0.349	0.04	-0.02
			350 K isotherm			
349.941	19.610	251.685	0.071	0.028	0.12	-0.55
349.940	19.007	244.049	0.070	0.029	0.13	-0.55
349.939	18.006	231.282	0.069	0.030	0.15	-0.54
349.938	17.002	218.364	0.067	0.031	0.16	-0.53
349.937	16.003	205.413	0.066	0.032	0.17	-0.51
349.936	15.002	192.363	0.064	0.033	0.18	-0.49
349.936	14.004	179.307	0.063	0.035	0.19	-0.47
349.937	13.001	166.136	0.061	0.037	0.19	-0.44
349.938	12.001	152.987	0.060	0.039	0.19	-0.41
349.937	11.002	139.860	0.058	0.042	0.19	-0.37
349.937	10.001	126.717	0.057	0.045	0.18	-0.34
349.938	9.000	113.615	0.055	0.049	0.17	-0.30

349.938	8.000	100.577	0.054	0.054	0.16	-0.26
349.936	7.002	87.645	0.052	0.060	0.15	-0.22
349.937	6.010	74.879	0.051	0.068	0.13	-0.18
349.938	5.000	61.978	0.049	0.080	0.11	-0.14
349.937	4.031	49.701	0.048	0.097	0.09	-0.11
349.937	2.989	36.636	0.047	0.127	0.08	-0.07
349.937	1.999	24.360	0.045	0.185	0.06	-0.03
349.938	0.999	12.096	0.044	0.362	0.03	-0.01
			375 K isotherm			
374.924	19.829	230.614	0.067	0.029	0.08	-0.43
374.925	19.006	221.282	0.066	0.030	0.09	-0.42
374.924	17.999	209.763	0.065	0.031	0.11	-0.42
374.922	17.000	198.252	0.064	0.032	0.12	-0.41
374.923	16.002	186.676	0.062	0.033	0.12	-0.39
374.922	14.999	174.971	0.061	0.035	0.13	-0.38
374.922	13.998	163.244	0.060	0.037	0.14	-0.36
374.922	12.999	151.487	0.058	0.039	0.14	-0.34
374.923	11.978	139.434	0.057	0.041	0.14	-0.31
374.922	11.000	127.886	0.056	0.044	0.14	-0.28
374.923	10.000	116.053	0.054	0.047	0.13	-0.26
374.922	9.000	104.240	0.053	0.051	0.12	-0.23
374.922	8.000	92.436	0.052	0.056	0.11	-0.20
374.922	6.999	80.668	0.050	0.062	0.10	-0.17
374.923	5.999	68.937	0.049	0.071	0.09	-0.14
374.924	4.999	57.260	0.048	0.083	0.08	-0.12
374.923	3.999	45.645	0.046	0.102	0.06	-0.09
374.924	2.984	33.935	0.045	0.133	0.05	-0.06

374.925	1.999	22.640	0.044	0.193	0.03	-0.04
374.923	0.998	11.262	0.042	0.377	0.02	-0.02

[a] Expanded uncertainties ($k = 2$): $U(p > 3)/\text{MPa} = 75 \cdot 10^{-6} \cdot \frac{p}{\text{MPa}} + 3.5 \cdot 10^{-3}$; $U(p < 3)/\text{MPa} = 60 \cdot 10^{-6} \cdot \frac{p}{\text{MPa}} + 1.7 \cdot 10^{-3}$; $U(T) = 4$ mK; $\frac{U(\rho)}{\text{kg·m}^{-3}} = 2.5 \cdot 10^{4} \frac{\chi_S}{\text{m}^3\cdot\text{kg}^{-1}} + 1.1 \cdot 10^{-4} \cdot \frac{\rho}{\text{kg·m}^{-3}} + 2.3 \cdot 10^{-2}$.

Table 7. Virial coefficients $B(T)$ and $C(T)$ and second interaction virial coefficient $B_{12}(T)$, with their expanded ($k = 2$) uncertainties, from the fit to the five experimental binary ($CO_2 + O_2$) mixtures studied in this work and part one of this study [1], at the average temperature of each isotherm.

T / K	B / $cm^3 \cdot mol^{-1}$	$U(B)$ / $cm^3 \cdot mol^{-1}$	C / $cm^6 \cdot mol^{-2}$	$U(C)$ / $cm^6 \cdot mol^{-2}$	B_{12} / $cm^3 \cdot mol^{-1}$	$U(B_{12})$ / $cm^3 \cdot mol^{-1}$	$10^2 (B_{12,exp} - B_{12,GERG})/B_{12,GERG}$	$10^2 (B_{12,exp} - B_{12,CG})/B_{12,CG}$
				(0.95 CO_2 + 0.05 O_2)				
299.947	-113.22	0.94	4474	365	-39.39	1.97	68.2	2.7
324.953	-93.82	0.28	3943	91	-30.83	0.81	59.2	-3.1
				(0.90 CO_2 + 0.10 O_2)				
299.924	-105.90	0.20	4294	40	-41.31	0.71	66.6	6.3
324.937	-87.07	0.19	3618	43	-29.65	0.69	45.1	-7.8
374.913	-61.23	0.32	2866	105	-19.37	0.87	53.2	-8.0
				(0.80 CO_2 + 0.20 O_2)				
299.947	-91.56	0.12	3746	21	-41.52	0.63	51.6	4.3
324.955	-75.35	0.20	3238	49	-32.65	0.71	45.6	-0.4
349.939	-62.69	0.62	2922	245	-26.14	1.38	45.7	-2.0
374.923	-52.12	0.49	2583	188	-19.96	1.15	43.6	-6.4
				(0.50 CO_2 + 0.50 O_2)				
275.007	-67.88	0.06	2747	8	-51.13	0.60	23.9	-0.8
299.946	-54.62	0.02	2376	2	-40.82	0.58	20.8	-3.4
324.952	-44.24	0.07	2132	11	-32.75	0.60	19.6	-4.9
349.935	-35.79	0.21	1929	56	-25.96	0.72	18.8	-6.4
374.921	-28.77	0.25	1778	74	-20.21	0.77	18.6	-8.2
				(0.25 CO_2 + 0.75 O_2)				
250.027	-51.28	0.20	2030	41	-63.39	0.71	10.2	-4.7
260.026	-46.82	0.05	1956	6	-58.75	0.59	11.0	-4.0
274.996	-40.58	0.06	1827	8	-51.65	0.59	10.5	-4.4

299.942	-31.90	0.09	1655	17	-41.61	0.61	9.7	-5.2
324.952	-24.84	0.14	1523	32	-33.36	0.65	9.1	-6.0
349.938	-19.16	0.14	1438	32	-26.85	0.65	10.2	-5.5
374.923	-14.25	0.31	1343	98	-20.98	0.86	10.1	-6.4

Table 8. Parameters of the interpolation of the second interaction virial coefficient $B_{12}(T)$ for the binary (CO_2 + O_2) system as a function of temperature using Eq. (8)

Parameter	Value ± expanded (k = 2) uncertainty	Unit
N_0	68.8 ± 3.0	$cm^3 \cdot mol^{-1}$
N_1	-33100 ± 820	$cm^3 \cdot mol^{-1} \cdot K$
RMS of residuals	2.3	%

Table 9. Statistical analysis of the experimental (p, ρ, T) data set with respect to the GERG-2008 EoS (density residuals), EOS-CG (density residuals), and virial EoS (pressure residuals) for the five (CO_2 + O_2) mixtures studied in this work and the previous one [1], including literature data for comparable mixtures. AAD = absolute average deviation, Bias = average deviation, RMS = root mean square deviation, MaxD = maximum deviation.

Reference[a]	$x(O_2)$	N[b]	Covered ranges		Experimental *vs* GERG-2008				Experimental *vs* EOS-CG				Experimental *vs* virial EoS	
			T / K	p / MPa	AAD / %	Bias / %	RMS / %	MaxD / %	AAD / %	Bias / %	RMS / %	MaxD / %	RMS / %	MaxD / %
This study, part one [1]	0.050321	45	275-375	0.5-8	0.29	0.28	0.45	1.5	0.077	-0.0022	0.11	0.41	0.035	0.10
This study, part one [1]	0.099856	47	260-375	0.5-9	0.69	0.68	1.1	4.4	0.15	0.054	0.26	1.2	0.047	0.16
This study, part one [1]	0.199907	70	250-375	0.5-13	1.3	1.3	1.9	6.6	0.22	-0.052	0.50	3.2	0.47	3.4
This work	0.499973	123	250-375	0.5-20	1.1	1.1	1.4	3.9	0.59	-0.58	0.90	3.0	0.22	1.3
This work	0.749914	151	250-375	0.5-20	0.32	0.31	0.40	1.1	0.66	-0.66	0.90	2.6	0.062	0.44
Gururaja et al. [46]	0.0-1.0	9	297-303	0.1	1.8	-1.7	3.3	7.6	1.8	-1.7	3.3	7.6	3.6	8.2
Mantovani et al. [40][c]	0.060700	96	303-383	1-20	1.4	-1.4	2.0	8.3	2.1	-2.1	2.8	13	8.0	22

Mantovani et al. [40][c]	0.129100	100	303-383	1-20	2.2	-2.2	2.8	13	3.5	-3.5	4.1	13	4.1	15
Mazzoccoli et al. [45]	0.044200	12	273-293	1-7	2.4	2.4	2.9	6.7	1.8	1.8	2.5	6.6	1.9	5.4
Mazzoccoli et al. [45]	0.148800	18	273-293	1-7	1.2	0.4	1.8	5.2	1.9	-0.89	2.5	7.2	1.5	2.9
Al-Siyabi [42]	0.050000	26	323-423	8-40	1.3	-1.1	1.5	3.0	1.5	-1.5	1.7	3.2	9.1	19
Commodore et al. [53]	0.01246	112	324-400	2-35	0.17	0.094	0.26	1.2	0.15	0.0033	0.23	1.2	11	24
Muirbrook [54]	0.035-0.4	32	273.15	Saturation	43	38	75	247	39	34	70	235	22	44

[a] Only measurements in the vapor and supercritical phase have been considered.

[b] Number of experimental points.

[c] Used for the development of EOS-CG.